

On the nonexistence of degenerate phase-shift multibreathers in a zigzag Klein-Gordon model

T. Penati^a, V. Koukouloyannis^b, M. Sansottera^a, P.G. Kevrekidis^c, S. Paleari^a

^a*Department of Mathematics “F.Enriques”, Milano University, via Saldini 50, Milano, Italy, 20133*

^b*Department of Mathematics, Statistics and Physics, College of Arts and Sciences, Qatar University, P.O. Box 2713, Doha, Qatar*

^c*Department of Mathematics and Statistics, University of Massachusetts, Amherst, MA 01003-4515, USA*

Abstract

In this work, we study the existence of low amplitude four-site phase-shift multibreathers for small values of the coupling ϵ in Klein-Gordon (KG) chains with interactions longer than the classical nearest-neighbour ones. In the proper parameter regimes, the considered lattices bear connections to models beyond one spatial dimension, namely the so-called zigzag lattice, as well as the two-dimensional square lattice. We examine initially the persistence conditions of the system, in order to seek for vortex-like waveforms. Although this approach provides useful insights, due to the degeneracy of these solutions, it does not allow us to determine if they constitute true solutions of our system. In order to overcome this obstacle, we follow a different route. In the case of the zigzag configuration, by means of a Lyapunov-Schmidt decomposition, we are able to establish that the bifurcation equation for our model can be considered, in the small energy and small coupling regime, as a perturbation of a corresponding non-local discrete nonlinear Schrödinger (NL-dNLS) equation. There, nonexistence results of degenerate phase-shift discrete solitons can be demonstrated by exploiting the expansion of a suitable density current of the NL-dNLS, obtained in recent literature. Finally, briefly considering a one-dimensional model bearing similarities to the square lattice, we conclude that the above strategy is not efficient for the proof of the existence or nonexistence of vortices due to the higher degeneracy of this configuration.

1. Introduction

The study of nonlinear dynamical lattices of Klein-Gordon, as well as Fermi-Pasta-Ulam and related types has received considerable attention over the past two decades due to the intense interest in waveforms which are exponentially localized in space and periodic in time, namely the so-called discrete breathers [7, 16]. These states have been recognized as emerging rather generically in systems that combine discreteness and nonlinearity. Relevant experimental examples abound and range from Josephson junction arrays [41, 5] to electrical transmission lines [14], from micro-mechanical cantilever arrays [39, 38] to coupled torsion pendula [11], and from coupled antiferromagnetic layers [40] to granular crystals [6, 9], to name just a few examples.

Most of these studies concern fundamental localized states, and most of them are predominantly in simpler, more controllable one-dimensional settings [16]. However, optical [28], atomic [20] and other settings suggest an interest in exploring higher-dimensional settings. In the latter, novel structures (such as discrete vortices, also referred to as phase-shift multibreathers) emerge [10, 12] and occasional surprises arise, such as the existence of energy thresholds for breather existence [15] or the potential of higher charge vortices to be more stable than their lower charge counterparts under appropriate conditions [21]. It has been argued that (as will also be discussed further below) suitable adaptations of beyond-nearest-neighbor interactions [23] and the so-called zigzag [13] chains share some of the intriguing features of higher-dimensional settings, while remaining effectively one-dimensional in their formulation. For this reason, the latter will represent the starting point for our study in what follows.

More specifically, in this work, we are interested in Klein-Gordon (KG) models with range of interactions beyond nearest-neighbour, with Hamiltonian

$$\mathcal{H} = \sum_{j \in \mathbb{Z}} \left[\frac{1}{2} y_j^2 + V(x_j) \right] + \sum_{j \in \mathbb{Z}} \sum_{h=1}^r \epsilon_h \frac{(x_{j+h} - x_j)^2}{2},$$

where $V(x_j) = \frac{1}{2} x_j^2 + \frac{1}{4} x_j^4$. This Hamiltonian describes an infinite chain of anharmonic oscillators with linear interactions between them up to r neighbours and vanishing boundary conditions at infinity $\lim_{n \rightarrow \pm\infty} x_n = \lim_{n \rightarrow \pm\infty} y_n = 0$, which are automatically satisfied since we set $\ell^2(\mathbb{R}) \times \ell^2(\mathbb{R})$ as the phase space of the system. We will denote by E the energy of the system, i.e. the (conserved along the dynamics) value of the Hamiltonian.

In what follows we will limit our analysis to range of interaction $r = 3$. By considering $\epsilon_j = k_j \epsilon$, with $k_1 = 1$, the above Hamiltonian becomes

$$\begin{aligned} \mathcal{H} &= \mathcal{H}_0 + \epsilon \mathcal{H}_1 = \\ &= \sum_{j \in \mathbb{Z}} \left(\frac{y_j^2}{2} + V(x_j) \right) \\ &\quad + \frac{\epsilon}{2} \sum_{j \in \mathbb{Z}} [(x_j - x_{j+1})^2 + k_2 (x_j - x_{j+2})^2 + k_3 (x_j - x_{j+3})^2]. \end{aligned} \tag{1}$$

We are interested in the existence, in the small coupling limit (i.e., for values of the coupling close to the anti-continuum limit [29] of $\epsilon \rightarrow 0$), of multibreather solutions. These constitute a class of periodic orbits whose energy is spatially localized on few oscillators (or sites). More precisely, in this paper we

focus on solutions localized on four adjacent oscillators (namely with indices $j \in S = \{1, 2, 3, 4\}$), for a reason that will be clear in a while. If, in the uncoupled case $\epsilon = 0$, they are given the same energy (or action), any orbit is periodic (having the oscillators moving with the same frequency), irrespectively of the phase differences between them, forming in this way a completely resonant four-dimensional torus. Our investigation can thus be seen to fall within the general question of the perturbation of low-dimensional resonant tori in Hamiltonian dynamics.

When we consider only nearest neighbours interactions in (1), i.e., setting $k_2 = k_3 = 0$, it is well known that only multibreathers with *standard phase-differences* ($\varphi = 0$ or π) between adjacent oscillators survive the breaking of the resonant torus [24]. If next-to-nearest (or longer range) neighbour interactions are added, other solutions with non-standard phase differences may survive: these are called *phase-shift* multibreathers (see e.g. [26, 35]). The emergence of phase-shift multibreathers in both one-dimensional KG and dNLS models with interactions longer than these of the nearest-neighbours interactions, have been investigated in some recent literature [23, 19, 8]. This issue partially overlaps with the study of vortex structures in two-dimensional lattices, like in [32, 12, 22]. Indeed, a suitable long-range interaction in a one-dimensional lattice allows to re-

produce the local interactions involved in a two-dimensional vortex, for example in a hexagonal or square lattice, thus providing an emulation of the two-dimensional object by a one-dimensional one at leading order in the coupling perturbation parameter ϵ ; such an approximation clearly fails at higher orders, due to the differences in terms of lattice shape and interaction among sites.

A special case of a two-dimensional lattice is the so-called zigzag lattice [13]. This lattice consists of just two oscillator chains which are connected as shown in Fig. 1. In this case, we can easily see that *vortex* solutions of Fig. 1 correspond to *four-site* multibreathers in the system of Fig. 2. The zigzag system is described by a Hamiltonian

$$\mathcal{H}_{110} = \sum_{j \in \mathbb{Z}} \left(\frac{1}{2} y_j^2 + V(x_j) \right) + \frac{\epsilon}{2} \sum_{j \in \mathbb{Z}} [(x_{j+1} - x_j)^2 + (x_{j+2} - x_j)^2], \quad (2)$$

that corresponds to a Hamiltonian (1) with $k_2 = 1$ and $k_3 = 0$. Indeed, the subscript of \mathcal{H} refers to the values of the coupling constants k (including k_1 which is always 1 in our notation).

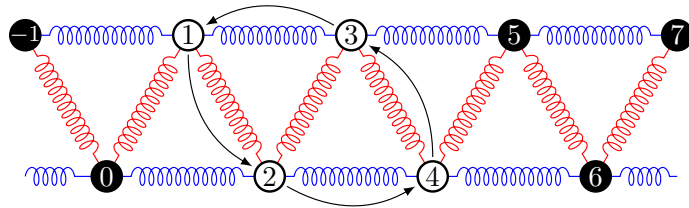


Figure 1: The two-dimensional zigzag model: all the interactions are nearest neighbor ones with the same strength. The indexing indicates the energy flow of the vortex solutions. Color online.

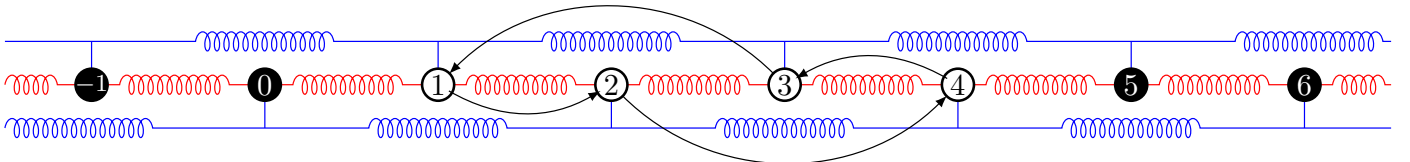


Figure 2: The corresponding one-dimensional zigzag model. The numbers indicate the correspondance to the two-dimensional zigzag model. Color online.

Both in the one-dimensional and in the two-dimensional case, the existence of multibreathers is typically performed via implicit function theorem arguments, which rely on the non-degeneracy of some linearized equation. This is the case, for example, of the classical result in [1], where true multibreather solutions are obtained from approximate solutions which correspond to critical points of an averaged (effective) Hamiltonian: in this context, an approximate solution has to satisfy some *persistence conditions* (see e.g. [23]) which select admissible candidates of phase-differences for a possible continuation. The same analytical tool, i.e., the implicit function theorem, can be used also in a different scheme: approaching the original problem with a Lyapunov-Schmidt decomposition (with the torus being resonant), it is used to solve the Range equation, and then the use of some symmetry, like time-reversibility, can remove the Kernel directions (see [35]). However, in some degenerate cases, the candidate solutions we acquire from the

persistence conditions do not correspond to true solutions of our systems. In such cases, a deeper analysis is required which typically involves higher order terms of the bifurcation (kernel) equation.

By studying the persistence conditions for the zigzag system (2), we realize that the candidate vortex solutions of Fig.1 are not isolated, but appear as two one-parameter families within the three-dimensional manifold of phase-differences. These two families intersect in what we call *symmetric vortex* configuration, since it features the standard vortex phase differences $\Phi^{(sv)} \equiv \varphi = \pm(\pi/2, \pi, -\pi/2)^1$, where $\varphi \equiv (\varphi_1, \varphi_2, \varphi_3)$, see (6).

¹The reason that the $\Phi^{(sv)}$ configuration is the one with $\pm(\pi/2, \pi, -\pi/2)$ and not the $\pm(\pi/2, \pi/2, \pi/2)$ as one could have expected, is that, as we can see from Fig.1 the vortex-flow is $1 \rightarrow 2 \rightarrow 4 \rightarrow 3 \rightarrow 1$ while the phase differences are calculated using consecutive oscillators.

On the other hand, we will call all the other solutions of these two families, with $\varphi \neq \Phi^{(sv)}$ as *asymmetric vortices*. Let us note here that these families also include some of the standard ($\varphi_i \in \{0, \pi\}$) multibreather solutions in addition to the isolated standard solutions of the persistence conditions.

Due to the degeneracy, which manifests itself into the presence of families of candidate solutions, and even more in their intersection points, we attempt to complement our analysis by performing a numerical investigation of the persistence conditions of the full problem (1) in the neighbourhood of the values $(k_2, k_3) = (1, 0)$, which correspond to the zigzag configuration. In this study, we realize first of all that there exist families² of solutions which are non-degenerate and consequently easily continued to real solutions. In addition, there is a solution family at $k_2 = 1$ for all values of k_3 . As $k_3 \rightarrow 0$, we observe that some of the non-degenerate families geometrically converge also to the $k_2 = 1$ family increasing in this way the degeneracy and for $k_3 = 0$ they become the two vortex families of solutions. Thus, it is difficult to get a definitive answer on the existence of true vortex solutions in the case of the Hamiltonian \mathcal{H}_{110} only by the study of the persistence conditions.

To get a complete description of the continuation we thus follow a different route, exploiting the corresponding dNLS model

$$H_{110} = \sum_j |\psi_j|^2 + \frac{3}{8} \sum_j |\psi_j|^4 + \frac{\epsilon}{2} \sum_j [|\psi_{j+1} - \psi_j|^2 + |\psi_{j+2} - \psi_j|^2], \quad (3)$$

as a bridge to \mathcal{H}_{110} . Indeed the former can be shown to be a good approximation of the latter in the energy regime $E \ll 1$ and for couplings $\epsilon \ll \sqrt{E}$ (see, e.g., [3, 34] or Subsection 3.3). Moreover, although the system H_{110} shares the same degeneracy as the original KG model, we are able to more straightforwardly derive the nonexistence of any phase-shift discrete soliton of H_{110} following the scheme of [37] by exploiting the expansion of an invariant quantity, i.e., the *Density Current*. Since this efficient nonexistence strategy is based on some minimal smoothness assumption with respect to ϵ , to get nonexistence assuming only continuity, we also expand the bifurcation equation at leading orders showing that this H_{110} case is less degenerate than the one studied in [37]. This weaker degeneracy allows to deduce nonexistence of the continuation by verifying a sufficient condition on the linearized bifurcation equation. Since this sufficient condition is robust under small perturbation, we are then able to transfer the nonexistence result of H_{110} to the original system \mathcal{H}_{110} , showing the *nonexistence* of any vortex solution (symmetric or asymmetric) for the degenerate model (2), in the prescribed regime of the two main parameters E and ϵ . We may claim that the nonexistence result itself, in the presence of degeneracy, and the above mentioned indirect strategy here applied, represents the key point of the paper.

In order to state such a result (which can be found in Section 3 in a slightly more technical formulation), we introduce the four-dimensional resonant torus filled by periodic orbits, belonging to the possible solutions of \mathcal{H}_{110} for $\epsilon = 0$

$$\bar{u}_j(\tau) = \begin{cases} 0, & j \notin S \\ x(\tau + \theta_j), & j \in S \end{cases}, \quad (4)$$

²Since now we consider the persistence conditions of the full problem (1), the families are considered in the (k_2, k_3) -space.

where $S = \{1, 2, 3, 4\}$ and $x(\tau)$ is a nonlinear oscillation of

$$\gamma^2 x'' + x + x^3 = 0, \quad x(0) = \rho, \quad (5)$$

where $\tau := \gamma t$ is the rescaled time induced by the frequency γ associated to the (small) amplitude ρ of the oscillation, and φ_j are phase differences between the above mentioned (which are also called as “central”) successive oscillators with

$$\varphi_j := \theta_{j+1} - \theta_j, \quad j \in S^* = \{1, 2, 3\}. \quad (6)$$

We have then

Theorem 1.1. *For ϵ small enough ($\epsilon \neq 0$), the only four-site unperturbed solutions (4) that can be continued, at fixed frequency γ , to solutions $u_j(\rho, \epsilon, \tau)$ of (2), correspond to $\varphi_j \in \{0, \pi\}$.*

Moreover, in all the cases which appear to be non-degenerate, the “dNLS approximation” strategy, allows to derive any existence result for (1) from the existence result for the corresponding dNLS model

$$H = \sum_j |\psi_j|^2 + \frac{3}{8} \sum_j |\psi_j|^4 + \frac{\epsilon}{2} \sum_j [|\psi_{j+1} - \psi_j|^2 + k_2 |\psi_{j+2} - \psi_j|^2 + k_3 |\psi_{j+3} - \psi_j|^2], \quad (7)$$

and provides explicit (though not sharp) estimates of the approximation of asymmetric vortices in (1) with the corresponding phase-shift discrete solitons in (7) (cf. with Theorem 2.1 of [3]).

The price one has to pay for the use of this strategy lies in the restrictions in the regime of parameters for which the models (1) are well approximated by the corresponding averaged normal forms (7). However, Hamiltonian normal form theory provides the tools needed to modify the approximating models in different regimes of the parameters E and ϵ , as in [30, 34], thus leading to a new dNLS-type starting model for an indirect approach. Such a new nonlocal dNLS normal form would surely include additional linear and nonlinear corrections with respect to those present in (7). We conclude this section by remarking that there exist even more degenerate models within the family (1). One of these is the Hamiltonian \mathcal{H}_{101} (see (14)) which has $k_2 = 0$ and $k_3 = 1$ and it is used for the study of vortex-like configurations in two-dimensional square lattices. This system admits, at the level of the persistence condition, three vortex families, having the symmetric vortex configuration in their triple intersection, giving thus a complete degeneration. We stress that the corresponding dNLS model is exactly the one studied in [37], but within the scheme implemented in the present paper, the higher degeneration of \mathcal{H}_{101} does not allow us to transfer the nonexistence result proved in [37] to the corresponding KG chain. We are presently exploring a different normal form strategy which works directly on the original KG model and interpret the problem in the classical sense of breaking of a completely resonant low-dimensional torus [36].

This paper is structured as follows. The numerical explorations are reported in Section 2, where we perform a study of the persistence conditions of both the zigzag (2) and the \mathcal{H}_{101} system as well as of the full system (1) in the (k_2, k_3) -parameter values neighborhood which correspond to the zigzag

and the \mathcal{H}_{101} systems. The mathematical strategy and the main nonexistence result for the KG model (2) is given in Section 3, while in Section 4 we use the first order expansion of the Density Current and the sufficient condition on the linearized bifurcation equation in order to prove nonexistence of vortex solutions in the zigzag-dNLS system (3). Finally, Section 5 includes some concluding remarks about possible future directions on the topic.

2. Study of the persistence conditions

In the present Section we investigate the possibility of existence of multibreather solutions by following a procedure similar to the one introduced in [23] using the results of [25, 27, 26], and by numerical calculations.

2.1. The zigzag system

The *persistence conditions* for the zigzag system are the equations that provide the candidate configurations among the ones in the anticontinuous limit $\epsilon = 0$, that could be continued, for ϵ nonzero but small enough, to provide multibreather solutions for this system. These equations are derived through an averaging procedure which is described in [23] and the main points will be presented in what follows. For $\epsilon = 0$, we consider four “central” oscillators moving (with the same frequency but arbitrary initial phases) while the rest lie at their equilibrium. The motion of each one of these central oscillators is described by the cosine Fourier expansion

$$x(w, J) = \sum_{n=1}^{\infty} A_{2n-1}(J) \cos[(2n-1)w], \quad (8)$$

where (J, w) refer to the action-angle variables for the single oscillator while the lack of the even terms A_{2n} in the Fourier expansion stems from the symmetry of the potential V .

Since we want to study structures with four central oscillators, only three phase differences φ_i between them are defined as in (6). It has been proven in [1] that the configurations $\boldsymbol{\varphi} = (\varphi_1, \varphi_2, \varphi_3)$ that could be continued for $\epsilon \neq 0$ to provide multibreather solutions correspond to critical points of the *effective Hamiltonian*, which at first order of approximation is given by $\mathcal{H}^{\text{eff}} = \mathcal{H}_0(J_i) + \epsilon \langle \mathcal{H}_1 \rangle(\varphi_i, J_i)$. The average value of the coupling term of the Hamiltonian (1) $\langle \mathcal{H}_1 \rangle$ is calculated along the unperturbed orbit and reads

$$\begin{aligned} \langle \mathcal{H}_1 \rangle = & -\frac{1}{2} \sum_{m=1}^{\infty} A_m^2 \left(\cos(m\phi_1) + \cos(m\phi_2) + \cos(m\phi_3) + \right. \\ & + k_2 (\cos(m(\phi_1 + \phi_2)) + \cos(m(\phi_2 + \phi_3))) \\ & \left. + k_3 \cos(m(\phi_1 + \phi_2 + \phi_3)) \right). \end{aligned}$$

The persistence conditions are obtained from the relation $\frac{\partial \langle \mathcal{H}_1 \rangle}{\partial \varphi_i} = 0$ and for the case of the zigzag system (2), i.e., with $k_2 = 1$ and $k_3 = 0$, read

$$\mathcal{P}_{110}(\boldsymbol{\varphi}) \equiv \begin{cases} M(\varphi_1) + M(\varphi_1 + \varphi_2) = 0 \\ M(\varphi_2) + M(\varphi_1 + \varphi_2) + M(\varphi_3 + \varphi_2) = 0 \\ M(\varphi_3) + M(\varphi_2 + \varphi_3) = 0 \end{cases} \quad (9)$$

with

$$M(\varphi) \equiv \sum_{m=1}^{\infty} (2m-1) A_{2m-1}^2 \sin((2m-1)\varphi), \quad (10)$$

with A_i as in (8).

Note that, in the dNLS case, the conditions (9) hold but with

$$M(\varphi) \equiv \sin(\varphi), \quad (11)$$

due to the rotational symmetry of the model, i.e., only the first Fourier mode contributes.

Taking under consideration the symmetries of $M(\phi)$

$$\begin{aligned} M(\pi + \varphi) &= -M(\varphi), & M(-\varphi) &= -M(\varphi) = M(2\pi - \varphi), \\ M(\pi - \varphi) &= +M(\varphi), & M(0) &= M(\pi) = 0, \end{aligned}$$

it is straightforward to check that the persistence conditions both for the zigzag-KG case, i.e., (9) and (10), as well as the zigzag-dNLS case, i.e., (9) and (11), admit two families of solutions

$$F_1 : \boldsymbol{\varphi} = (\varphi, \pi, -\varphi), \quad F_2 : \boldsymbol{\varphi} = (\varphi, \pi, \pi + \varphi), \quad (12)$$

in addition to the other four standard isolated solutions $F_{\text{iso}} = \{(0, 0, 0), (0, 0, \pi), (\pi, 0, 0), (\pi, 0, \pi)\}$. In principle, all combinations of 0's and π 's work trivially, since the persistence conditions simply vanish. We have to note here that the rest of the standard multibreather solutions are part of the F_1 and F_2 families.

It is important to stress that conditions (9) are necessary but not sufficient for the existence of multibreather solutions. Indeed, in order to continue to real solutions of (2), the corresponding Jacobian matrix $D_{\varphi}(\mathcal{P})$ needs to be non-degenerate. The matrix $D_{\varphi}(\mathcal{P}_{110})$ is given by

$$\begin{pmatrix} M'(\varphi_1) + M'(\varphi_1 + \varphi_2) & M'(\varphi_2) + M'(\varphi_1 + \varphi_2) + M'(\varphi_2 + \varphi_3) & 0 \\ M'(\varphi_1 + \varphi_2) & M'(\varphi_2 + \varphi_3) & M'(\varphi_2 + \varphi_3) \\ 0 & M'(\varphi_2 + \varphi_3) & M'(\varphi_3) + M'(\varphi_2 + \varphi_3) \end{pmatrix},$$

where $M'(\varphi) \equiv \sum_{m=1}^{\infty} (2m-1)^2 A_{2m-1}^2 \cos((2m-1)\varphi)$. By using the symmetries of $M'(\varphi)$

$$\begin{aligned} M'(2\pi - \varphi) &= M'(\varphi) = M'(-\varphi), \\ M'(\pi - \varphi) &= M'(\pi + \varphi) = -M'(\varphi), \\ M'\left(\frac{3\pi}{2}\right) &= M'\left(\frac{\pi}{2}\right) = 0, \end{aligned}$$

it is easy to check that for the isolated solutions F_{iso} the matrix $D_{\varphi}(\mathcal{P}_{110})$ is non-degenerate so these solutions will be continued for $\epsilon \neq 0$ to provide multibreathers.

On the other hand, for the F_1, F_2 families, which correspond to asymmetric vortices, $D_{\varphi}(\mathcal{P}_{110})$ is degenerate possessing one zero eigenvalue, reflecting the freedom of these solutions with respect to variations in φ . So, we cannot know if these solutions are also true multibreather solutions of the system.

In particular, for the configurations where the two families cross each other and correspond to the two symmetric vortices, i.e., $\boldsymbol{\varphi} = \pm \Phi^{(\text{sv})} \equiv \pm(\pi/2, \pi, -\pi/2)$, the matrix $D_{\varphi}(\mathcal{P}_{101})$ reads

$$D_{\varphi}(\mathcal{P}_{101})|_{\Phi^{(\text{sv})}} = \begin{pmatrix} 0 & 0 & 0 \\ 0 & M'(\pi) & 0 \\ 0 & 0 & 0 \end{pmatrix}.$$

This means that its degeneracy is even higher since the dimension of its kernel is exactly two, i.e., given by the tangent directions to the two independent families in the vortex solutions.

2.2. The full system close to $k_2 = 1, k_3 = 0$

Given the above analysis, it seems interesting to study the role of the two families F_1 and F_2 of vortex solutions of the persistence conditions as the full system (1) tends to the zigzag model (2). This occurs close to the $(k_2, k_3) = (1, 0)$ point of the k -parameter space.

The persistence conditions of the full system (1) read

$$\mathcal{P}(\varphi) \equiv \begin{cases} M(\varphi_1) + k_2 M(\varphi_1 + \varphi_2) + k_3 M(\varphi_1 + \varphi_2 + \varphi_3) = 0 \\ M(\varphi_2) + k_2 M(\varphi_1 + \varphi_2) + k_2 M(\varphi_3 + \varphi_2) \\ \quad + k_3 M(\varphi_1 + \varphi_2 + \varphi_3) = 0 \\ M(\varphi_3) + k_2 M(\varphi_2 + \varphi_3) + k_3 M(\varphi_1 + \varphi_2 + \varphi_3) = 0 \end{cases} \quad (13)$$

where M is defined as in (10).

The proper illustration of the solutions of (13) would require a three-dimensional plot for every phase-difference φ_i as a function of both k_2 and k_3 . Since this surface is difficult to be properly illustrated, we prefer to present some sections, first for fixed k_3 , varying k_2 , and then by reversing the roles between k_2 and k_3 .

2.2.1. The $k_3 < 0$ case

A representative bifurcation diagram of this parameter region is shown in Fig. 3 where the solutions of the persistence conditions (13) are depicted for $k_3 = -0.001$ and $0.8 \leq k_2 \leq 1.2$. In this diagram all the solution families are shown, where we can distinguish both standard and phase-shift configurations. The family of solutions $F_1 : \varphi = (\varphi, \pi, -\varphi)$, discussed in Section 2.1 (see (12)), exists also for the persistence conditions of the full system for every value of k_3 and $k_2 = 1$ as it is easy to realize by substituting the values of φ which correspond to F_1 into (13). This family is depicted as a vertical line at $k_2 = 1$ in the top panel of Fig. 3. In this diagram another phase-shift solution family is shown which lies close to $\varphi_{1,3} = \pi, \varphi_2 = 0$. This family is not related to vortex solutions in the sense that it does not converge to any of the F_1 or F_2 families as $(k_2, k_3) \rightarrow (1, 0)$: indeed, for $F_{1,2}$ one has $\varphi_2 = \pi$. On the contrary it remains almost invariant in the parameter region under consideration.

2.2.2. The $k_3 \geq 0$ case

A representative example of this parameter region is depicted in Fig. 4 for $k_3 = 0.01$. We observe here that two new phase-shift families appear, bifurcating from the symmetric vortex configuration $\varphi = \Phi^{(sv)} = (\pi/2, \pi, -\pi/2)$, as will become more transparent through our parametric variations below. Indeed, in order to acquire a better understanding of the bifurcating families, in Fig. 5 we perform a magnification of the area around the bifurcation point, for the values of k_3 close to zero. Each family is determined by its values of φ_i 's and it is detailed in Table 1 (e.g., family 1 consists of the $\varphi_1 = \textcircled{1}, \varphi_2 = \textcircled{2}, \varphi_3 = \textcircled{2}$ in Fig. 5, etc.).

In this sequence of figures we can see that the bifurcation points of the phase-shift families under consideration approach $\Phi^{(sv)}$ and the families themselves tend to coincide with the F_2 family (12) as $k_3 \rightarrow 0$. For $k_3 = 0$ the families coincide with F_2 which visually coincides also with F_1 . The F_1 and F_2 families really cross each other at $\Phi^{(sv)}$.

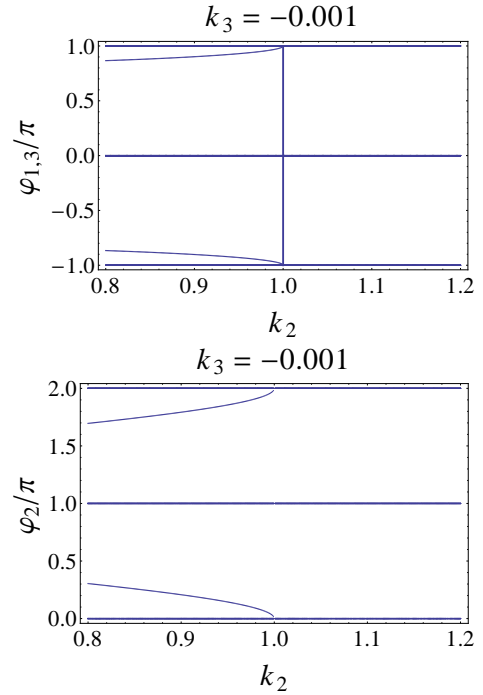


Figure 3: The complete bifurcation diagrams for $k_3 = -0.001$. In this diagrams all the solution families are shown. There are no vortex-related families for $k_3 < 0$ except the F_1 one which exists for every k_3 .

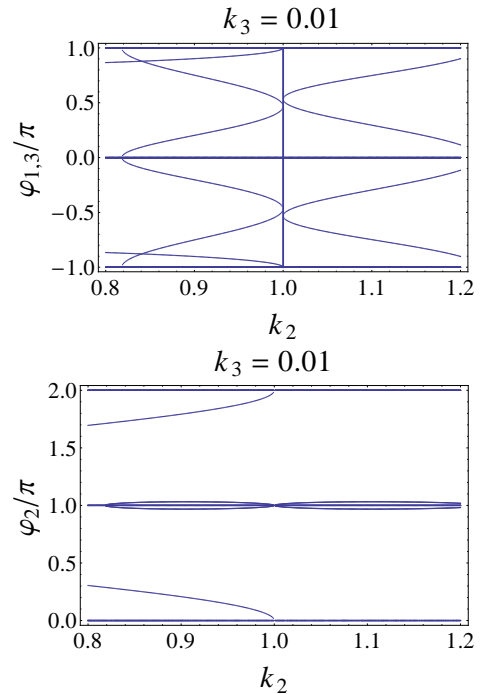


Figure 4: The complete bifurcation diagrams for $k_3 = 0.01$. In addition to the already existing families which for $k_3 < 0$, in the $k_3 \geq 0$ case two more phase-shift appear, which bifurcate from $\varphi = \Phi^{(sv)}$ (see also the figures below).

# of Family	Branch description		
	φ_1	φ_2	φ_3
1	①	②	②
2	②	①	①
3	③	③	④
4	④	④	③

Table 1: The solution families depicted in Fig. 5.

This is also suggested in Fig. 6, where the role of k_2 and k_3 has been reversed. Here, k_2 has been chosen close to, but less than, 1 and k_3 left free to vary around 0. The two families which are depicted in Fig. 6 are the ones shown in Table 2. We can observe in a more clear way the difference between the $k_3 \leq 0$ case and the $k_3 > 0$ case, in terms of phase-shift solutions. When $k_3 > 0$ there are branches connecting (apparently) to 0 and π : although the situation very close to $k_3 = 0$ is not perfectly shown, it is anyway evident that the branches in the upper and lower parts of the frames get closer and closer as $k_2 \rightarrow 1$, like converging to a curve which emerges from $\Phi^{(sv)}$. At exactly $k_2 = 1$, one should observe a full band for the phase differences $\varphi_{1,3}$. The picture is completely symmetrical to the one of Fig. 6 in the $k_2 > 1$ case.

# of Family	Branch description		
	φ_1	φ_2	φ_3
1	①	②	①
2	②	①	②

Table 2: The solution families depicted in Fig. 6.

The overall picture emerging from the above numerical exploration is the following. Whenever $k_2 \neq 1$, solutions appear to be isolated, thus non-degenerate and suitable to be continued. Nonetheless, as $k_2 \rightarrow 1$, their non-degeneration gets weaker and weaker, so that the domain of continuation in the coupling parameter ϵ is expected to vanish, according to the standard estimate given by the implicit function theorem. The degenerate scenario which appears at $k_2 = 1$, due to the existence of a one-parameter family of solutions F_1 for generic values of k_3 , becomes richer at $k_3 = 0$, since a second family F_2 arises which intersects the already existing F_1 at $\Phi^{(sv)}$. The possibility to continue such degenerate solutions requires a more accurate mathematical analysis, that we develop in the forthcoming Sections 3 and 4.

2.3. The \mathcal{H}_{101} system

Before entering the more mathematical part of the paper, in the present section we will study the persistence conditions of the \mathcal{H}_{101} model, i.e., the model (1) with $k_2 = 0$ and $k_3 = 1$ which is described by the Hamiltonian

$$\mathcal{H}_{101} = \sum_{j \in \mathbb{Z}} \left(\frac{1}{2} y_j^2 + V(x_j) \right) + \frac{\epsilon}{2} \sum_{j \in \mathbb{Z}} [(x_{j+1} - x_j)^2 + (x_{j+3} - x_j)^2]. \quad (14)$$

Such a system represents a first order approximation of a square NN lattice and a four-site multibreather solution of (14) can be thought of as representing a one-dimensional analogue of a four-site vortex for the two-dimensional square KG lattice and as it will be shown it constitutes a more degenerate case than the one of the \mathcal{H}_{110} model.

In order to begin our investigation, we consider the persistence conditions for this system, which, following again [23], are given by

$$\mathcal{P}_{101}(\boldsymbol{\varphi}) \equiv \begin{cases} M(\varphi_1) + M(\varphi_1 + \varphi_2 + \varphi_3) = 0 \\ M(\varphi_2) + M(\varphi_1 + \varphi_2 + \varphi_3) = 0 \\ M(\varphi_3) + M(\varphi_1 + \varphi_2 + \varphi_3) = 0 \end{cases} \quad (15)$$

where $M(\varphi)$ is given by (10). The corresponding NL-dNLS system

$$H_{101} = \sum_j |\psi_j|^2 + \frac{3}{8} \sum_j |\psi_j|^4 + \frac{\epsilon}{2} \sum_j [|\psi_{j+1} - \psi_j|^2 + |\psi_{j+3} - \psi_j|^2], \quad (16)$$

has been the subject of a detailed investigation performed in [37]. Note that (16) possesses the same persistence conditions (15) but with $M(\varphi) \equiv \sin(\varphi)$, see (11). In [37], it is showed that Eqs. (15) and (11) admit three families of *asymmetric vortex* solutions

$$\begin{aligned} F_1 : \boldsymbol{\varphi} &= (\varphi, \varphi, \pi - \varphi), \\ F_2 : \boldsymbol{\varphi} &= (\varphi, \pi - \varphi, \varphi), \\ F_3 : \boldsymbol{\varphi} &= (\varphi, \pi - \varphi, \pi - \varphi), \end{aligned} \quad (17)$$

in addition to the two isolated standard solutions $F_{\text{iso}} : \boldsymbol{\varphi} = \{(0, 0, 0), (\pi, \pi, \pi)\}$. Again, the rest of the standard configurations of this case are part of the F_1, F_2, F_3 families. By using the symmetries of $M(\varphi)$, it is easy to prove that also the persistence equations (15) and (10) admit the same families of solutions. These families are degenerate since the corresponding Jacobian $D_{\boldsymbol{\varphi}}(\mathcal{P}_{101})$ possesses a zero eigenvalue, while the *symmetric vortex* solutions

$$\Phi_{101}^{(sv)} \equiv \boldsymbol{\varphi} = \pm \left(\frac{\pi}{2}, \frac{\pi}{2}, \frac{\pi}{2} \right)$$

are fully degenerate, since $D_{\boldsymbol{\varphi}}(\mathcal{P}_{101})$ equals the null matrix. The latter can be seen both by a direct computation, or by observing that in these solutions we have three independent Kernel directions, one for each family passing through the solution.

2.4. The full system close to $k_2 = 0, k_3 = 1$

In order to understand how the three above families merge, we numerically study the persistence of the full problem (1) in the region of the parameter point $(k_2, k_3) = (0, 1)$ around the $\Phi_{101}^{(sv)}$ configuration. Since we consider low amplitude solutions the results for the two models (Klein-Gordon and dNLS) are equivalent both qualitatively as well as quantitatively, since the differences in the solutions are negligible³.

In order to showcase the relevant results, we consider first some specific values of k_3 (close to 1) and we perform a scan for solutions in an interval of k_2 (close to 0) and then we reverse the roles of k_2 and k_3 .

³This fact holds of course also for the \mathcal{H}_{110} model studied before.

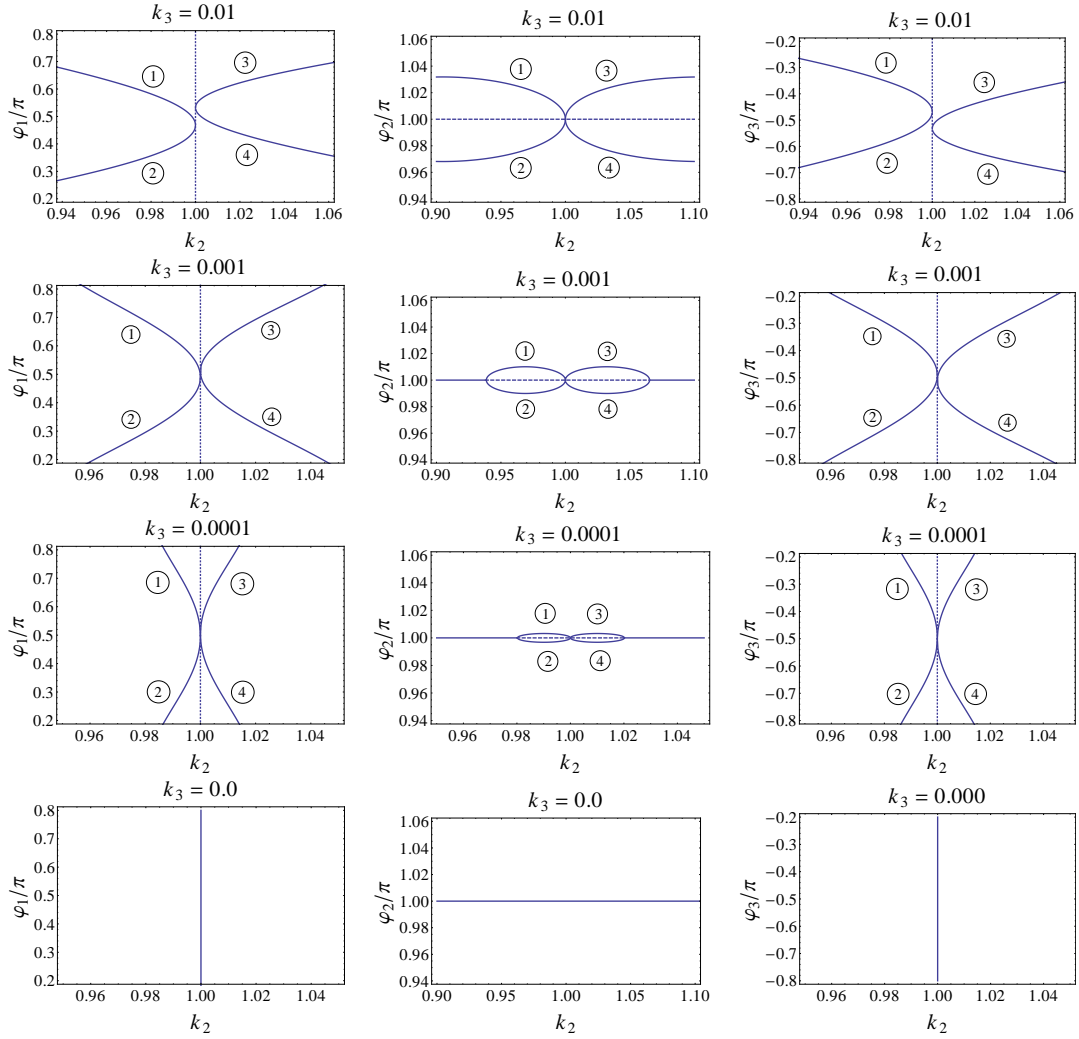


Figure 5: The bifurcation diagrams in the neighborhood $k_2 = 1$ and $\varphi = \Phi^{(sv)}$ are shown, for $k_3 = 0.01, 0.001, 0.0001, 0$, respectively. The family $F_1 : \varphi = (\varphi, \pi, -\varphi)$ is degenerate (possesses one 0 eigenvalue) and it is represented by a dotted line at $k_2 = 1$.

2.4.1. The $k_3 < 1$ case

In order to examine this parameter region we consider the values $k_3 = 0.9, 0.99$ and 0.999 . The corresponding solution families are shown in Fig. 7. In the top row the values of the angles φ_1 and φ_3 are shown while the bottom row depicts the values of φ_2 . Although, the φ_1 and φ_3 angles are depicted in the same diagram, this does not mean that $\varphi_1 = \varphi_3$ for every value of k_2 . The four families which are shown in Fig. 7 are labeled with encircled numbers and are summarized in Table 3 below (e.g., family 1 is defined as $\varphi_1 = \textcircled{1}$ of the upper row of the figure, $\varphi_2 = \textcircled{1}$ of the lower row and $\varphi_3 = \textcircled{2}$ of the upper row panels). We see in these diagrams how these families converge to the $k_2 = 0$ asymptote. In particular, families 1 and 4 converge to F_3 , while families 2 and 3 converge to F_1 (17). The different line symbols denote different linear stability of the families. In particular a solid line corresponds to a family with one unstable eigenvalue while the dashed line corresponds to two unstable eigenvalues. As the families converge one of their stability eigenvalue converges to zero and it changes sign when k_2 crosses zero. Since the stability discussion lies outside the scope of the present manuscript we will not refer further to these facts.

# of Family	Branch description		
	φ_1	φ_2	φ_3
1	$\textcircled{1}$	$\textcircled{1}$	$\textcircled{2}$
2	$\textcircled{2}$	$\textcircled{1}$	$\textcircled{1}$
3	$\textcircled{3}$	$\textcircled{2}$	$\textcircled{4}$
4	$\textcircled{4}$	$\textcircled{2}$	$\textcircled{3}$

Table 3: The solution families depicted in Fig. 7.

2.4.2. The $k_3 > 1$ case

The bifurcation-diagram for this case is depicted in Fig. 8. We can clearly observe that families 1 and 4 of Table 4 below converge into F_3 as $k_3 \rightarrow 1$ while families 2 and 3 converge to F_1 . The main difference of this diagrams, with respect to the ones of the $k_3 < 1$ case, is that in this case there exist also the two new phase-shift solution families 5 and 6, where the families 1-4 bifurcate from through pitchfork bifurcations. These families have also the characteristic that they are the only ones that exist for $k_2 = 0$ and for all $k_3 > 0$.

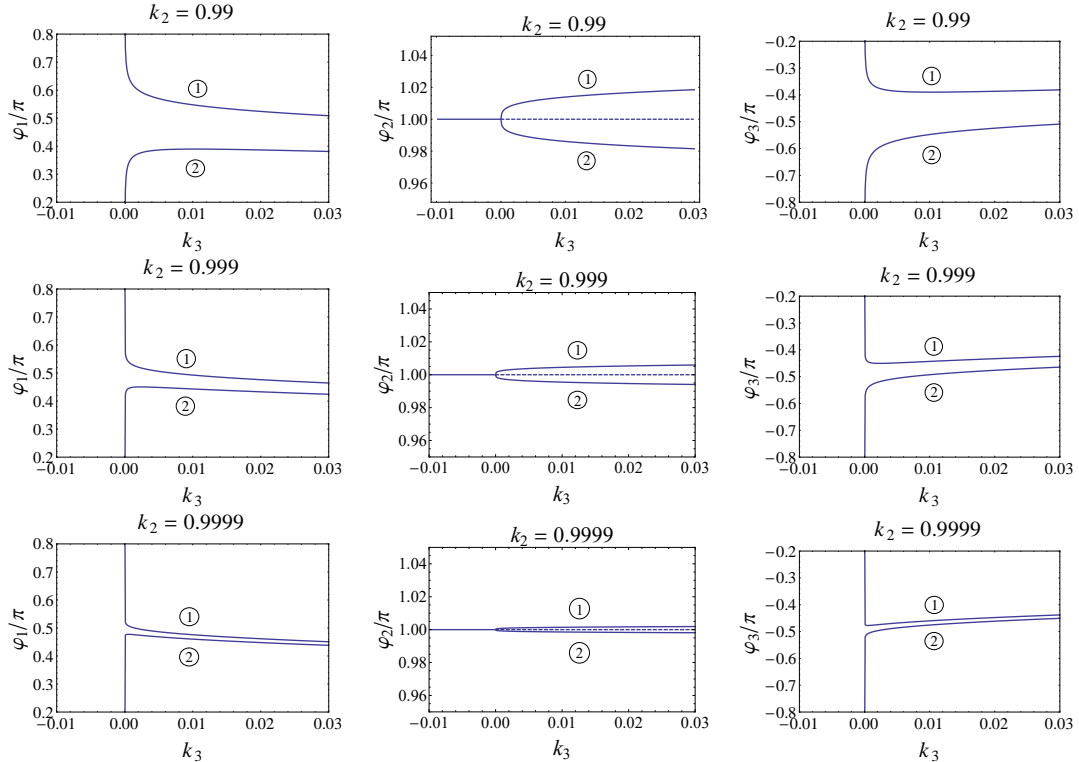


Figure 6: The bifurcation diagrams are shown, for three different values of k_2 close to 1, respectively $k_2 = 0.99, 0.999$ and 0.9999 .

# of Family	Branch description		
	φ_1	φ_2	φ_3
1	①	①	②
2	②	①	①
3	③	②	④
4	④	②	③
5	⑤	③	⑤
6	⑥	④	⑥

Table 4: The solution families depicted in Fig. 8.

2.4.3. The $k_3 = 1$ case

For $k_3 = 1$, the Jacobian is highly degenerate and hence we show no frame for this value of k_3 . Nevertheless, it is straightforward to see that the three families F_1, F_2 and F_3 coincide at $k_3 = 1$.

In order to demonstrate this fact better, as well as to better show the role of the families 5 and 6 of the $k_3 > 1$ case, we reverse that role of k_2 and k_3 in the diagrams.

2.4.4. The $k_2 \neq 0$ case

We consider now specific values of k_2 close to $k_2 = 0$ (i.e., $k_2 = -0.001, -0.0001, 0.0001, 0.001$) and an interval of values around $k_3 = 1$. We numerically seek for solutions of the persistence conditions (13) and the results are shown in Fig. 9. First of all we can see the family $F_2 : \varphi = (\varphi, \pi - \varphi, \varphi)$ which exists for $k_3 = 1$ and every value of k_2 . Since this family is degenerate it is depicted as a dotted line. The rest of the fam-

ilies depicted there are shown in Table 5 below. We can see that families 1 and 4 tend to F_1 while families 2 and 3 tend to F_3 as $k_2 \rightarrow 0$. Geometrically this means that both tend to the $k_3 = 1$ asymptote. On the other hand, there exist families 5 and 6 which correspond to the families 5 and 6 of Fig. 8. We see that they exist only for $k_3 \geq 1$ being a product of a saddle-node bifurcation occurring at $k_3 = 1$. Although these are k_2, k_3 -parameter solution families for (13), they constitute an isolated solution of Eqs. (15).

# of Family	Branch description		
	φ_1	φ_2	φ_3
1	①	①	②
2	②	①	①
3	③	②	④
4	④	②	③
5	⑤	③	⑤
6	⑥	④	⑥

Table 5: The solution families depicted in Fig. 9.

2.4.5. The $k_2 = 0$ case

To complement the picture set forth in the previous subsections, we separately consider the special case $k_2 = 0$. For this value of k_2 the only families that exist for $k_3 \neq 0$ are the families 5 and 6 of Fig. 9 as it can be shown better in Fig. 8. The resulting bifurcation diagram is shown in Fig. 10 since for this particular case it holds that $\varphi_1 = \varphi_2 = \varphi_3$.

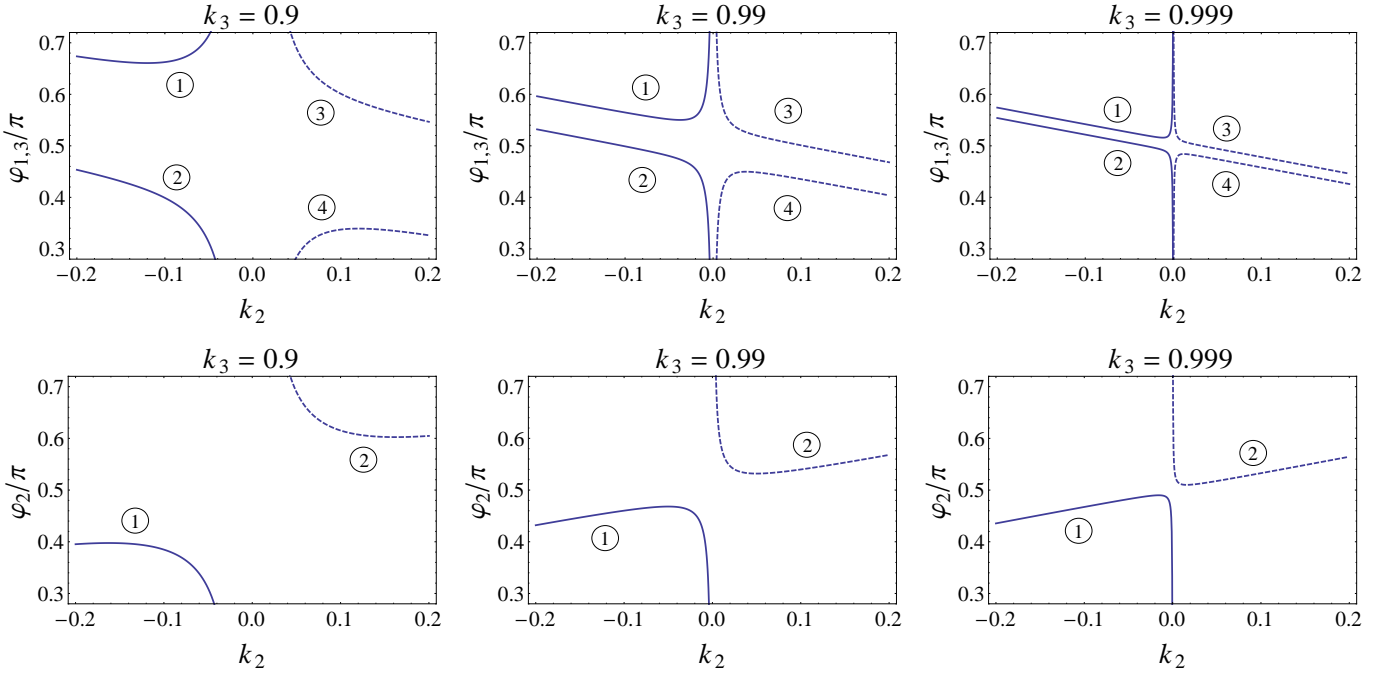


Figure 7: The bifurcation diagrams in the neighborhood $k_2 = 0$, $\varphi_i = \pi/2$ are shown, for $k_3 = 0.9, 0.99$ and 0.999 . We can observe how the various solution families converge to the $k_2 = 1$ asymptote.

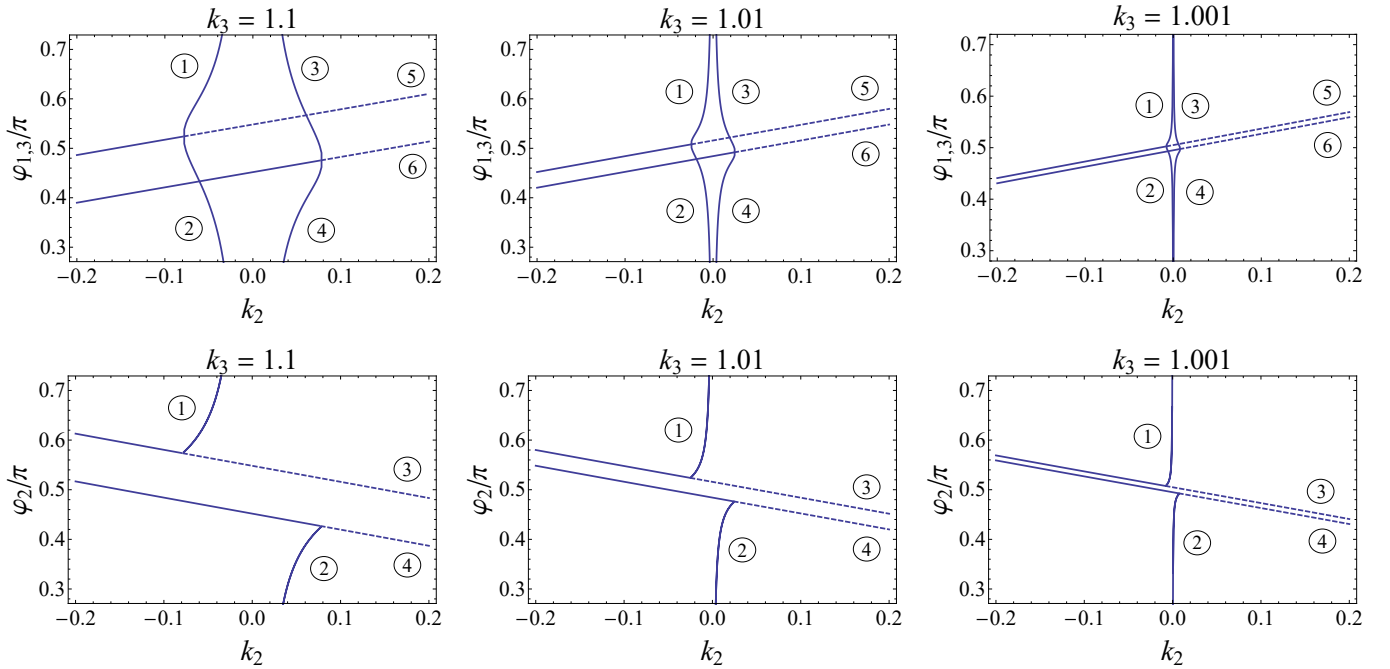


Figure 8: The bifurcation diagrams in the neighborhood $k_2 = 0$, $\varphi_i = \pi/2$ are shown, for $k_3 = 1.1, k_3 = 1.01$ and 1.001 . As $k_3 \rightarrow 1$ The families converge to the vortex families as $k_3 \rightarrow 1$.

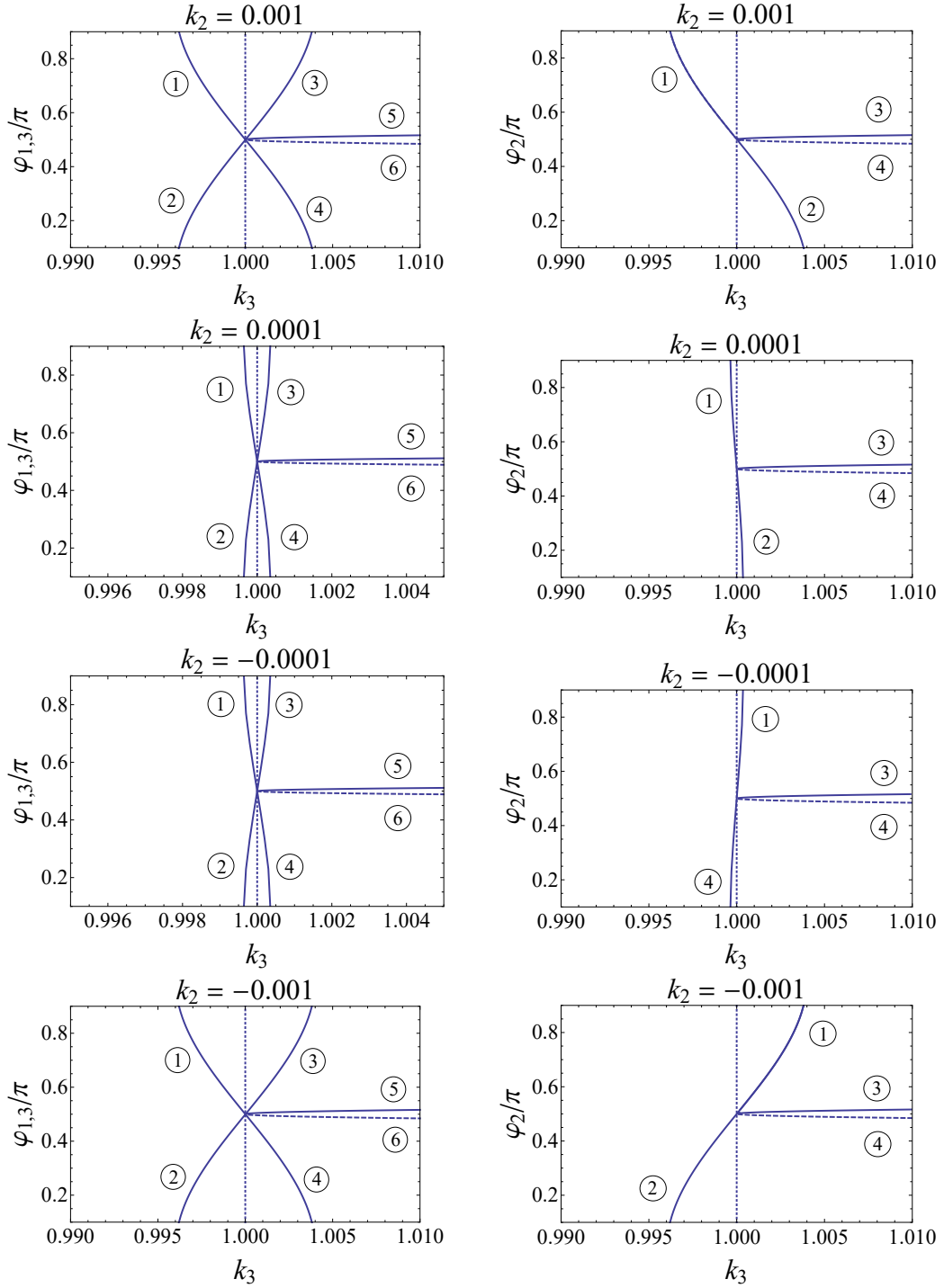


Figure 9: The bifurcation diagrams in the neighborhood $k_3 = 0$ and $\varphi = \Phi^{(sv)}_{101}$ are shown, for $k_2 = -0.001, -0.0001, 0.0001, 0.001$, respectively. The family $F_2 : (\varphi, \pi - \varphi, \varphi)$ is degenerate and it is represented by a dotted line at $k_3 = 1$.

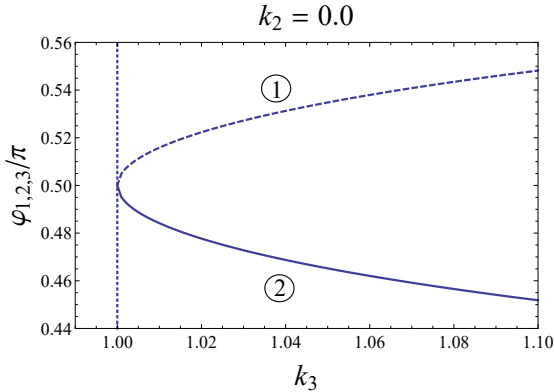


Figure 10: The bifurcation diagram for $k_2 = 0$ in the neighborhood $k_3 = 1$, $\varphi_i = \pi/2$ is shown.

The fact that for this choice of k_2 and for $k_3 = 1$ we get the symmetric vortex solution $\Phi_{101}^{(sv)}$ both as a member of the vertical families and as a member of the “parabolic” family, numerically poses the question of the existence of the symmetric vortex solution in the real system. This question is also triggered by the fact that the two-dimensional analogue of our system in the dNLS limit it has been proven to support vortex solutions [32].

We summarize the results of the previous numerical investigation, by saying that the persistence conditions provide three one-parameter families of candidate MBs, instead of the two families for the \mathcal{H}_{110} case. Each family carries two standard in-phase/out-of-phase solutions (whose existence is guaranteed via other approaches,[35]) and the three intersect in two highly symmetric objects, having $\varphi = \Phi_{101}^{(sv)}$ and emulating two-dimensional vortices. The same kind of scenario and consequent degeneracy is shared by its non-local discrete NLS (NL-dNLS) approximation

$$H_{101} = \sum_j |\psi_j|^2 + \frac{3}{8} \sum_j |\psi_j|^4 + \frac{\epsilon}{2} \sum_j [|\psi_{j+1} - \psi_j|^2 + |\psi_{j+3} - \psi_j|^2], \quad (18)$$

examined systematically in [37]. It is thus natural to attempt transferring the nonexistence results there obtained to the corresponding \mathcal{H}_{110} model, by means of an accurate mathematical analysis. However, the techniques developed in the present paper in the subsequent sections are tailored for less degenerate models. More comments on this are reported in Section 3.6.

3. The zigzag KG model

Motivated by the numerical results detailed in Section 2, we present here a complete description of the problem of continuing, from the anti-continuous limit $\epsilon = 0$, the phase shift solutions obtained from the persistence condition (9), thus focusing on the zigzag model (2). We first develop a Lyapunov-Schmidt decomposition (see [2]), which enables to link time-periodic solutions of the general class of KG models (1) to time-periodic solutions of the corresponding resonant normal forms (7); there the continuation problem can be formulated, and solved, in a simpler way due to the rotational symmetry. To relate (1)

with (7) we follow essentially the scheme developed in [3]. The proof will be divided in several steps, the last one illustrated in a separated Section. Here we will also provide the more detailed version of Theorem 1.1; the corresponding statements (Theorems 3.1 and 3.2) are presented after the first step of the proof in order to make reference to the objects introduced at that stage. In particular, Theorem 3.1 is formulated for the general class of Hamiltonians (1), while Theorem 3.2 applies in the restricted context of the zigzag KG model (2) and its normal form (3).

Let us consider the KG Hamiltonian (1) and its equations of motion

$$\ddot{x}_j = -x_j - x_j^3 + \epsilon(Lx)_j, \quad (19)$$

with

$$L := \Delta_1 + k_2 \Delta_2 + k_3 \Delta_3, \\ (\Delta_m x)_j := x_{j-m} - 2x_j + x_{j+m}.$$

We look for a periodic orbit with frequency γ ; hence by introducing the time scaling $u_j(\tau) := x_j(t)$, where $\tau := \gamma t$, we get

$$\gamma^2 u'' + u + u^3 - \epsilon L u = 0. \quad (20)$$

We define

$$L_0 := \gamma^2 \partial_\tau^2 + \mathbb{I}, \quad L_\epsilon := L_0 - \epsilon L, \quad N(u) := u^3. \quad (21)$$

The equation for a generic periodic orbit becomes

$$\mathcal{F}(\epsilon, u) := L_\epsilon u + N(u) = 0, \quad (22)$$

with

$$\mathcal{F} : \mathbb{R} \times X_2 := H^2([0, 2\pi], \ell^2) \rightarrow X_0 := L^2([0, 2\pi], \ell^2),$$

where $X_{0,2}$ are endowed with the usual norms (see Sections 3.2 and 3.3 of [3]).

As it is stated in the Introduction, we consider, in the unperturbed case $\epsilon = 0$, a periodic orbit $\bar{u}(\tau)$ which lies on the four-dimensional completely resonant torus (4) with amplitude ρ (see (5)). We wish to continue this periodic orbit for $\epsilon \neq 0$, thus we look for a function $u(\rho, \epsilon, \tau)$ such that $u(\rho, 0, \tau) = \bar{u}(\tau)$ and (22) is solved for ϵ small enough

$$\mathcal{F}(\epsilon, u(\rho, \epsilon, \tau)) = 0, \quad |\epsilon| < \epsilon^*(\rho), \quad (23)$$

with γ kept fixed.

The problem has been partially solved in [35] by restricting to time-reversible solutions $u(-\tau) = u(\tau)$; i.e., by considering only standard phase-differences $\varphi_j = \{0, \pi\}$ for all $j \in S$. Indeed, with this strategy the problem reduces to non-degenerate critical points where the implicit function theorem can be applied, like in the averaging approach of [1, 26, 25]. In the case of other phase-differences, like the vortex (or phase-shift multi-breather) solutions we consider here, it is not possible to make such a restriction, which ensures invertibility of the linearized operator $\mathcal{F}_u(0, \bar{u})$ on the subspace of even periodic solutions. In other words, in our case, the approximate solution \bar{u} is a degenerate critical point; thus a small perturbation may in principle

destroy the solution. In order to see that the linearized operator $\mathcal{F}_u(0, \bar{u})$ has a non-trivial Kernel, let us recall some facts presented in the first part of [35]⁴.

First, notice that

$$\mathcal{F}_u(0, \bar{u})[\zeta] = \begin{cases} L_0 \zeta_j & j \notin S, \\ L_0 \zeta_j + 3\bar{u}^2(\tau)_j \zeta_j & j \in S. \end{cases}$$

The non-resonant condition $j\gamma \neq \pm 1$ allows to invert L_0 on the space of 2π -periodic functions. On the other hand, differentiating the nonlinear oscillation equation w.r.t. both τ and the energy E , one sees that

$$\text{Ker}(\gamma^2 \partial_\tau^2 + 3x^2(\tau + \varphi_j)) = \left\langle x'(\tau + \varphi_j), \tau \frac{\partial \gamma}{\partial E} x'(\tau + \varphi_j) \right\rangle;$$

as a consequence, the non-degeneracy condition of the frequency $\frac{\partial \gamma}{\partial E} \neq 0$ guarantees that only the time derivatives $x'(\tau + \varphi_j)$ are 2π -periodic solutions. Thus the differential $\mathcal{F}_u(0, \bar{u})$ has a four-dimensional Kernel

$$\text{Ker}(\mathcal{F}_u(0, \bar{u})) = \langle f_j(\tau) \rangle, \quad j \in S,$$

generated by the velocities of the nonlinear oscillations⁵

$$f_j = [0|x'(\tau + \varphi_j)|0].$$

For the above reason an implicit function theorem cannot be applied, unless (as in [35]) we restrict⁶ to $\varphi_j \in \{0, \pi\}$, and a Lyapunov-Schmidt decomposition represents a natural approach to the problem.

3.1. The first Lyapunov-Schmidt decomposition

We consider (20) and we introduce the time-Fourier expansion for the solution of the uncoupled anharmonic oscillator $x(\tau)$ in (5)

$$x(\tau) = \sum_{k \geq 1} a_k \cos(k\tau); \quad (24)$$

then, from (4), we get

$$\bar{u}_j(\tau) = \begin{cases} 0 & j \notin S \\ \sum_{k \geq 1} a_k \cos(k\tau + k\varphi_j) & j \in S \end{cases},$$

thus we can write $\bar{u}_j = \sum_{k \geq 1} a_k (\cos(k\varphi_j) \cos(k\tau) - \sin(k\varphi_j) \sin(k\tau))$, for any $j \in S$. Let us now introduce the Fourier base

$$e_k(\tau) = \begin{cases} \cos(k\tau) & k \geq 0 \\ -\sin(k\tau) & k < 0 \end{cases}; \quad (25)$$

⁴ Geometrically, the main idea is that a small displacement on the four-dimensional torus from a given unperturbed periodic solution, leads to a new unperturbed periodic solution with the same frequency.

⁵ We will use the notation $[\dots, \cdot, \cdot, \cdot, \cdot, \dots]$ to denote values along the chain: in particular, the two vertical bars enclose the sites belonging to S .

⁶ Indeed, let us set $u(\tau) := x'(\tau + \pi)$. Using 2π periodicity of $x(\tau)$ and its even-parity we immediately get $u(-\tau) = x'(-(\tau + \pi)) = -x'(\tau + \pi) = -x'(\tau + \pi) = -u(\tau)$. Hence the velocities $x'(\tau + \varphi_j)$ are not even functions, i.e., the Kernel is transversal to the subspace of even solutions.

we can decompose $u \in \ell^2(\mathbb{R})$ in its Fourier components⁷

$$u(\tau) = \sum_{k \in \mathbb{Z} \setminus \{0\}} u_k e_k(\tau), \quad (26)$$

and introduce the Lyapunov-Schmidt decomposition⁸ which splits the first harmonics from the rest of the Fourier expansion

$$u = \mathbf{v} + \mathbf{w}, \quad \mathbf{v} = u_{-1} e_{-1}(\tau) + u_1 e_1(\tau); \quad (27)$$

in other words \mathbf{v} solves the harmonic oscillator equation $\frac{d^2 \mathbf{v}}{d\tau^2} + \mathbf{v} = 0$. We define

$$V_2 := \langle e_1, e_{-1} \rangle = \ker(\partial_\tau^2 + \mathbb{I}), \quad W_2 := V_2^\complement. \quad (28)$$

If we consider the unperturbed reference solution \bar{u} , we have for any $j \in S$

$$\bar{u}_j = \sum_{k \in \mathbb{Z}} \bar{u}_{j,k} e_k(\tau), \quad \bar{u}_{j,k} = \begin{cases} a_k \cos(k\varphi_j) & k > 0 \\ 0 & k = 0 \\ -a_k \sin(k\varphi_j) & k < 0 \end{cases},$$

thus we get

$$\bar{v}_j = a_1 \cos(\varphi_j) e_1(\tau) - a_1 \sin(\varphi_j) e_{-1}(\tau). \quad (29)$$

We rewrite the frequency as $\gamma^2 = 1 - \omega$. Indeed, in the small energy regime, the frequency γ is close to one, and its displacement ω is of order $\mathcal{O}(\rho^2)$. The equation (20) thus reads

$$\mathcal{F}(\epsilon, \mathbf{v}, \mathbf{w}) = L_\epsilon \mathbf{w} - \omega \mathbf{v} - \epsilon L \mathbf{v} + N(\mathbf{v} + \mathbf{w}) = 0. \quad (30)$$

When we project (30) on the Range $W_0 \subset X_0$ of $\partial_\tau^2 + \mathbb{I}$, and its complement V_0 , we get⁹

$$\begin{cases} \Pi_W \mathcal{F}(\epsilon, \mathbf{v}, \mathbf{w}) = L_\epsilon \mathbf{w} + \Pi_W N(\mathbf{v} + \mathbf{w}) = 0 & (R) \\ \Pi_V \mathcal{F}(\epsilon, \mathbf{v}, \mathbf{w}) = -\omega \mathbf{v} - \epsilon L \mathbf{v} + \Pi_V N(\mathbf{v} + \mathbf{w}) = 0 & (K) \end{cases}. \quad (31)$$

Proceeding as in Section 4 of [3], the Range equation (R), written as $\mathbf{w} = -L_\epsilon^{-1} \Pi_W N(\mathbf{v} + \mathbf{w})$, can be locally solved and approximated by $\tilde{\mathbf{w}}(\mathbf{v}, \epsilon)$

$$\tilde{\mathbf{w}}(\mathbf{v}, \epsilon) := -L_\epsilon^{-1} \Pi_W N(\mathbf{v}) = \mathcal{O}(\|\mathbf{v}\|_{X_2}^3),$$

with

$$\|\mathbf{w} - \tilde{\mathbf{w}}\|_{X_2} \leq C \|\mathbf{v}\|_{X_2}^5.$$

We move now to the Kernel equation (K), i.e., $-\omega \mathbf{v} - \epsilon L \mathbf{v} + \Pi_V(\mathbf{v} + \mathbf{w}(\mathbf{v}, \epsilon))^3 = 0$. Since $\mathbf{w}(\mathbf{v}) = \mathcal{O}(\|\mathbf{v}\|_{X_2}^3)$, we can expand

$$\begin{aligned} \Pi_V(\mathbf{v} + \mathbf{w}(\mathbf{v}, \epsilon))^3 &= \Pi_V(\mathbf{v})^3 + [\Pi_V(\mathbf{v} + \mathbf{w}(\mathbf{v}, \epsilon))^3 - \Pi_V(\mathbf{v})^3] \\ &= \Pi_V(\mathbf{v})^3 + \mathcal{O}(\|\mathbf{v}\|_{X_2}^5). \end{aligned}$$

⁷ We will always use the subscript k to denote the Fourier index, and the subscript j for the site index.

⁸ Please notice the use of the sans serif font for the present decomposition variables: \mathbf{v} and \mathbf{w} . From subsection 3.4, the letters v and w , with the usual font, will have a different meaning.

⁹ For an easier notation we drop the zero subscript in the projectors $\Pi_V \equiv \Pi_{V_0}$ and $\Pi_W \equiv \Pi_{W_0}$.

We compute explicitly the Kernel projection of the leading term of the nonlinear part. First we have, by definition

$$\Pi_V(\mathbf{v})^3 = \left(\frac{1}{2\pi} \int_0^{2\pi} v^3(\tau) \cos(\tau) d\tau \right) e_1 + \left(\frac{1}{2\pi} \int_0^{2\pi} v^3(\tau) \sin(\tau) d\tau \right) e_{-1},$$

and since, omitting the τ dependence, we have

$$v^3 = u_1^3 e_1^3 + 3u_1^2 u_{-1} e_1^2 e_{-1} + u_{-1}^3 e_{-1}^3 + 3u_1 u_{-1}^2 e_1 e_{-1}^2,$$

trigonometric formulas give immediately

$$\begin{aligned} \Pi_V(\mathbf{v})^3 &= \frac{3}{4} ((u_1^2 + u_{-1}^2) u_1 \cos(\tau) + (u_1^2 + u_{-1}^2) u_{-1} \sin(\tau)) \\ &= \frac{3}{4} (u_1^2 + u_{-1}^2) \mathbf{v}. \end{aligned} \quad (32)$$

By defining the remainder as

$$\mathcal{R}(\mathbf{v}, \epsilon) := \Pi_V(\mathbf{v} + \mathbf{w}(\mathbf{v}, \epsilon))^3 - \Pi_V(\mathbf{v})^3, \quad (33)$$

we can rewrite the Kernel equation as

$$-\omega \mathbf{v} - \epsilon L \mathbf{v} + \frac{3}{4} (u_1^2 + u_{-1}^2) \mathbf{v} + \mathcal{R}(\mathbf{v}, \epsilon) = 0. \quad (34)$$

The Kernel equation, due to its dimension (\mathbf{v} is a two-dimensional vector of sequences), is equivalent to the system

$$\begin{aligned} -\omega u_1 - \epsilon L u_1 + \frac{3}{4} (u_1^2 + u_{-1}^2) u_1 + \langle \mathcal{R}(\mathbf{v}, \epsilon), e_1 \rangle &= 0 \\ -\omega u_{-1} - \epsilon L u_{-1} + \frac{3}{4} (u_1^2 + u_{-1}^2) u_{-1} + \langle \mathcal{R}(\mathbf{v}, \epsilon), e_{-1} \rangle &= 0 \end{aligned}$$

Introducing the complex variable ϕ

$$\phi := u_1 + i u_{-1}, \quad (35)$$

equation (34) takes the form

$$-\omega \phi - \epsilon L \phi + \frac{3}{4} \phi |\phi|^2 + \mathcal{R}(\phi, \epsilon) = 0, \quad (36)$$

using again the letter \mathcal{R} to denote the corresponding term of (34). It turns out that in the small energy regime (i.e., for ρ small enough) (36) looks as a ρ^2 -perturbation of the NL-dNLS stationary problem

$$-\omega \phi - \epsilon L \phi + \frac{3}{4} \phi |\phi|^2 = 0; \quad (37)$$

in other words, the term $\mathcal{R}(\phi, \epsilon)$ can be treated as a perturbation. Moreover, since also the remainder \mathcal{R} is equivariant under the rotational symmetry and conjugation, the whole (36) actually represents the stationary equation for a non-local dNLS model. We are now ready to give more detailed statements; Theorem 1.1 can be seen as their corollary.

3.2. Reformulation of the main results

The first statement allows to derive an existence and approximation result for a solution of (20), $u(\rho, \epsilon, \tau)$, from the existence of a non-degenerate NL-dNLS solution $v(\epsilon, \tau')$, precisely

Theorem 3.1. *Let $\phi(\epsilon)$ be a non-degenerate ϵ -family of solutions for (37) and let $v(\epsilon, \tau')$ be the corresponding real solution in V_2 , see (28). Then, there exist E^* and ϵ^* and a constant C_1 , such that, for $E < E^*$ and $\epsilon < E \epsilon^*$, there exists a non-degenerate two parameter family $u(\rho, \epsilon, \tau)$, solutions of (22), which fulfills*

$$\|u(\rho, \epsilon, \cdot) - v(\epsilon, \cdot)\|_{X_2} < C_1 \rho^3. \quad (38)$$

Several remarks are in order:

- Theorem 3.1 applies to any discrete soliton solution of the dNLS model (7), which is obtained as isolated solution of the corresponding persistence condition via implicit function theorem. In particular, it applies to those standard phase-difference solitons of the model H_{110} (but also in the more degenerate case H_{101}) which do not belong to the 1-parameter families of solutions of (9), provided (11) holds.
- The true solution and its approximation are of order $\mathcal{O}(\rho) \sim \mathcal{O}(\sqrt{E})$, thus the bound (38) on their difference, being $\mathcal{O}(\rho^3)$, is meaningful.
- The non-degeneracy assumption in Theorem 3.1 for the NL-dNLS solution is related to the constrained Hessian $D^2 E_1(\phi(0))$, being E_1 the ϵ -depending part of the Hamiltonian (7) (see [17, 19, 33]). This condition is equivalent (through the variational formulation of (37)) to the non-degeneracy of the linearized bifurcation equation we will use in Proposition 3.1.
- The distinct time variables, i.e., τ and τ' , reflect the different frequencies of the two unperturbed reference solutions. Indeed, since the ϵ -continuation is performed at fixed frequency, the two solutions keep this frequency difference. The different time variables permit to normalize the period to 2π .

The second statement claims the nonexistence of four-site vortices in the zigzag case KG model (2), at least in the regime of small enough energy E :

Theorem 3.2. *For any $\varphi \in (0, 2\pi)$, $\varphi \neq \pi$, there exists $E^*(\varphi)$ such that, for $E < E^*$, the solutions (12) of (9) cannot be continued at $\epsilon \neq 0$.*

Here we also have to stress that:

- The nonexistence statement is based on the analogous result for the zigzag-dNLS model (3), where the impossibility to solve the linearized bifurcation equation is sufficient to conclude the proof. The same holds if the linearized bifurcation equation is slightly perturbed, which is exactly what happens in the model (2) if the energy E is taken small enough. This is discussed in Section 3.5.2.
- It turns out that $E^*(\varphi) \searrow 0$ as $\varphi \rightarrow 0, \pi$, in agreement with the fact that for $\varphi = \{0, \pi\}$ the four-sites MBs exist.
- Theorem 3.2 does not exclude that four-sites asymmetric vortices appear for $\epsilon > \epsilon^*(\rho, \varphi)$. It only claims that it does not exist a continuous (in ϵ) branch which locally arises at $\epsilon = 0$.

3.3. Approximation of the Kernel equation

Let us first remark the following;

Notation. *Since there are two small parameters, the coupling ϵ and the amplitude ρ (introduced in (5) in order to maintain a notation as similar as possible with the paper [37]), in what follows we will indicate the dependence with respect to ϵ as an argument of the related quantities, and the dependence on ρ (absent in [37]) as a subscript. We also stress that, where it will be clear from the context, the absence of the subscript ρ will mean $\rho = 0$, i.e., for a generic quantity Z_ρ we will set $Z \equiv Z_0$.*

At $\epsilon = 0$, we denote by v_ρ the unperturbed solution of (36), corresponding to the Kernel projection \bar{v} in (29)

$$v_j = a_1 \cos(\varphi_j) - ia_1 \sin(\varphi_j) = a_1 e^{-i\varphi_j}, \quad j \in S. \quad (39)$$

Recalling that $\mathcal{R}(v, \epsilon) = \mathcal{O}(\|v\|_{X_2}^5)$, introducing the vector field $X_N(\phi) := \frac{3}{4}\phi|\phi|^2$ and the following ρ -scaling

$$\phi =: \rho \tilde{\phi}, \quad \epsilon =: \rho^2 \tilde{\epsilon}, \quad \omega =: \rho^2 \tilde{\omega}, \quad (40)$$

and immediately *dropping the tildes*, equation (36) reads

$$\rho^3 \left[-\omega \phi - \epsilon L \phi + X_N(\phi) + \rho^2 \mathcal{R}_\rho(\phi, \rho^2 \epsilon) \right] = 0. \quad (41)$$

Thus we have shown that, in the small energy regime, i.e., for ρ small enough, equation (41) (equivalent to (36)) looks as a ρ^2 -perturbation of the NL-dNLS problem (37). We remark that also the first three terms in the square brackets depend on ρ , so that in the following we will systematically add the corresponding subscript; it has been omitted here to help the comparison with formula (37) and to emphasize that those terms, though depending on ρ , do not vanish with ρ , so that the last term in (41) is really a small correction.

Remark 3.1. *Starting from (41), ϵ won't be anymore exactly the KG coupling (remember we are dropping the tildes of the scaling (40)), but it will represent the coupling of the (perturbed) dNLS associated to the original KG.*

We introduce¹⁰ the scaled unperturbed solution of (41), v_ρ , (again *dropping the tildes*), that has amplitude $a_1/\rho = \mathcal{O}(1)$ and uniquely defines the frequency detuning ω_ρ from the harmonic frequency, namely

$$\omega_\rho = \frac{3}{4}|v_\rho|^2 + \rho^2 \frac{\mathcal{R}_\rho(v_\rho, 0)}{v_\rho}.$$

By definition, v has to solve the uncoupled NL-dNLS problem, i.e., (41) with $\epsilon = 0$ and $\rho = 0$,

$$-\omega v + \frac{3}{4}v|v|^2 = 0 \quad \Rightarrow \quad \omega = \frac{3}{4}R^2, \quad R := \lim_{\rho \rightarrow 0} \frac{a_1}{\rho} \neq 0.$$

Analyzing the leading order expansion of $a_1(\rho)$, we provide an estimate for the distance between the two unperturbed solutions, v_ρ and v in

Lemma 3.1. *There exists $\rho^* < 1$ and two constants C_0 and c_0 such that, for $\rho < \rho^*$, one has*

$$\|v_\rho - v\|_{\ell^2(\mathbb{C})} < C_0 \rho^2, \quad |\omega_\rho - \omega| < c_0 \rho^2. \quad (42)$$

¹⁰We will follow again paper [37], decomposing ϕ in a reference solution v and a correction w .

Once we focus on a particular solution v_ρ of the uncoupled problem, we ask for its continuation for $\epsilon \neq 0$; we thus look for a correction $w_\rho(\epsilon)$ around v_ρ , that is continuous in ϵ , namely

$$w_\rho(v_\rho, \epsilon) := \phi_\rho(\epsilon) - v_\rho, \quad \text{with} \quad w_\rho(v_\rho, 0) = 0,$$

so that $\phi_\rho(\epsilon)$ solves (41).

Inserting the above definition, and exploiting that v_ρ is a solution for $\epsilon = 0$, the Kernel equation (41) takes the form

$$0 = \mathcal{F}(v_\rho; w_\rho, \rho, \epsilon) := F(v; w, \epsilon) + \mathcal{R}(v_\rho; w_\rho, \rho, \epsilon), \quad (43)$$

where

$$\begin{aligned} F_\rho(v_\rho; w_\rho, \epsilon) &:= -\omega_\rho w_\rho - \epsilon L(v_\rho + w_\rho) \\ &\quad + [X_N(v_\rho + w_\rho) - X_N(v_\rho)] \\ \mathcal{R}(v_\rho; w_\rho, \rho, \epsilon) &:= [F_\rho(v_\rho; w_\rho, \epsilon) - F(v; w, \epsilon)] \\ &\quad + \rho^2 [\mathcal{R}_\rho(v_\rho + w_\rho, \epsilon) - \mathcal{R}_\rho(v_\rho, 0)] \end{aligned} \quad (44)$$

In contrast with (41), in (43) we have a term completely independent of ρ , i.e., $\mathcal{F}(v_\rho; w_\rho, \rho, \epsilon)|_{\rho=0} \equiv F(v; w, \epsilon)$, which is indeed the $\mathcal{O}(1)$ leading term in ρ of (37), and is the dNLS model analyzed in Section 4.

The usual strategy to solve the kernel equation is to probe the applicability of the implicit function theorem. Thus we consider the linear operator

$$\Lambda_\rho := (D_w \mathcal{F})(v_\rho; 0, \rho, 0). \quad (45)$$

Following the same arguments shown in [37] it is not difficult to check that Λ_ρ has a four-dimensional kernel which inhibits the application of the implicit function theorem.

3.4. The second Lyapunov-Schmidt decomposition

Given the above comment on the non-applicability of the implicit function theorem in the case of Λ_ρ , we have to proceed (as in the NL-dNLS case developed in [37]) with a Lyapunov-Schmidt decomposition of

$$w_\rho = k_\rho + h_\rho, \quad k_\rho \in \text{Ker}(\Lambda_\rho), \quad h_\rho \in \text{Range}(\Lambda_\rho).$$

The equation (43) then becomes

$$\begin{cases} \mathcal{F}_H(v_\rho; k_\rho + h_\rho, \rho, \epsilon) = 0 \\ \mathcal{F}_K(v_\rho; k_\rho + h_\rho, \rho, \epsilon) = 0 \end{cases},$$

where the subscripts H and K denote the corresponding projections over $\text{Range}(\Lambda_\rho)$ and $\text{Ker}(\Lambda_\rho)$, respectively. The Range equation $\mathcal{F}_H = 0$ can be solved locally by the implicit function theorem and provides

$$h_\rho = h_\rho(v_\rho; k_\rho, \epsilon); \quad (46)$$

inserting (46) into $\mathcal{F}_K = 0$ we get the **bifurcation equation**, redefining \mathcal{F}_K as

$$0 = \mathcal{F}_K(v_\rho; k_\rho, \rho, \epsilon) := \mathcal{F}_K(v_\rho; k_\rho + h(v_\rho, k_\rho, \epsilon), \rho, \epsilon), \quad (47)$$

where now

$$\mathcal{F}_K : \mathbb{R}^4 \times \mathbb{R} \times \mathbb{R} \rightarrow \mathbb{R}^4,$$

is defined once given the unperturbed reference solution v_ρ . The following lemmas allow us to then properly treat (47) as a ρ -perturbation of the corresponding bifurcation equation for its normal form (7).

Lemma 3.2. *The function $\mathcal{F}_K(v_\rho; k, \rho, \epsilon)$ is smooth in ρ and $\mathcal{F}_K(v; k, 0, \epsilon) = F_K(v; k, \epsilon)$,*

where F_K is the corresponding bifurcation equation for (7) defined in (44).

Proof: For the proof it is simply necessary to show that the Lyapunov-Schmidt decomposition commutes with the limit $\rho \rightarrow 0$. As already observed, if $\rho = 0$, then equation (43) reduces to $F(v; k, \epsilon) = 0$. For such an equation, the Lyapunov-Schmidt decomposition is performed with respect to the linear operator Λ_0 . The smoothness in ρ of all the involved functions (including the ρ -family of isomorphism between the spaces of the Lyapunov-Schmidt decompositions) concludes the proof. \square

A further important characterization of the Kernel projection of both \mathcal{F} and F is that they vanish with ϵ , so that it is possible to introduce

$$\begin{aligned} \mathcal{F}_K(v_\rho^*; k_\rho, \rho, \epsilon) &=: \epsilon P_\rho(v_\rho^*; k_\rho, \rho, \epsilon), \\ F_K(v^*; k, \epsilon) &=: \epsilon P(v^*; k, \epsilon). \end{aligned} \quad (48)$$

In [37] we checked the corresponding property by a direct calculation. Here we limit to remark that it has to be true since, when $\epsilon = 0$, it corresponds to the existence of the ‘‘coordinates’’ (k_ρ, h_ρ) describing the four-dimensional torus around the chosen v_ρ^* . The additional property we have here is the continuity with respect to ρ , i.e.,

$$\rho \rightarrow 0 \quad \Rightarrow \quad P_\rho(v_\rho^*; k_\rho, \rho, \epsilon) \rightarrow P(v^*; k, \epsilon) \quad (49)$$

which reduces to

$$P_\rho(v_\rho^*; k_\rho, \rho, \epsilon) = 0 \quad (50)$$

for which we look for local solutions $\|k_\rho(\epsilon)\| \ll 1$, with $|\epsilon| \ll 1$ and $|\rho| \ll 1$.

3.5. Continuation from the persistence conditions

We will now concentrate on those particular solutions of the uncoupled system which satisfy the persistence conditions, that we connote with a star superscript. In particular let \bar{u}^* be an unperturbed solution given by (4) whose phases θ_j satisfy the persistence conditions (9) and (10); then we denote by

$$v_\rho^* := \frac{1}{\rho}(\bar{u}_1^* + i\bar{u}_{-1}^*) \quad (51)$$

its unique rescaled projection on V_2 , according to (27),(35) and (40); as already noted in general, v_ρ^* solves (41) with $\epsilon = 0$. Since the whole previous construction is continuous in ρ , we also have that $v^* = \lim_{\rho \rightarrow 0} v_\rho^*$, and

$$v_j^* = \begin{cases} Re^{-i\theta_j}, & j \in S \\ 0, & j \notin S \end{cases},$$

where the phase-differences $\varphi_j = \theta_{j+1} - \theta_j$, introduced in (6), satisfy the corresponding NL-dNLS persistence conditions given by (9) and (11) Indeed, in the limit of vanishing amplitude, i.e., for $\rho \rightarrow 0$, the KG persistence condition (9) converges to the NL-dNLS persistence condition, (see (65)), in view of the exponential decay of the Fourier components.

At the present stage of our construction it is worth recalling that the persistence conditions take the form

$$P_\rho(v_\rho^*; 0, \rho, 0) = 0 \quad \text{and} \quad P(v^*; 0, 0) = 0,$$

respectively for the KG and dNLS cases, since by continuity the ‘‘correction’’ k has to vanish with ϵ .

3.5.1. Proof of Theorem 3.1

The first part of Theorem 3.1 follows from

Proposition 3.1. *Let v_ρ^* be as in (51). If the corresponding v^* is linearly non-degenerate, which means that the Linearized Bifurcation Equation*

$$\epsilon \partial_\epsilon P(v^*; 0, 0) + D_k P(v^*; 0, 0)[k] = 0,$$

can be uniquely solved (apart from the Gauge direction), then there exists ρ^ such that, for $|\rho| < \rho^*$ the same holds true for the ρ -perturbed Linearized Bifurcation Equation*

$$\epsilon \partial_\epsilon P_\rho(v_\rho^*; 0, \rho, 0) + D_k P_\rho(v_\rho^*; 0, \rho, 0)[k] = 0.$$

Hence, there exists $\epsilon^(\rho)$ such that, for $|\epsilon| < \epsilon^*$ the bifurcation equation (50) can be locally solved and*

$$\|k_\rho(\epsilon) - k(\epsilon)\| < C\rho^2. \quad (52)$$

Proof: the proof is based on the same ideas of Theorem C.1 of [3]. From the definitions (43), (44) and (48), and by exploiting (42) and the Lipschitz-continuity of P_ρ , it is possible to show that

$$P_\rho - P = \mathcal{O}(\rho^2).$$

The non-degeneracy of the Linearized Bifurcation Equation for the NL-dNLS model, which is equivariant under the action of the Gauge symmetry, can be translated into the condition that the Kernel of the four-dimensional squared matrix

$$D_k P_\rho(v^*, 0, \rho, 0)$$

is given only by the Gauge direction, being invertible in the three-dimensional orthogonal complement¹¹. As we remarked already, the whole bifurcation equation $P_\rho(v_\rho^*, k, \rho, \epsilon) = 0$ is still Gauge equivariant, hence invertibility isn’t lost under a continuous, and small enough, ρ^2 -perturbation. Hence also $D_k P_\rho(v_\rho^*, 0, \rho, 0)$ is invertible in the Gauge-orthogonal subspace and estimate (52) is a standard by-product of the implicit function theorem. \square

In order to conclude the proof of Theorem 3.1, we still have to show that estimate (38) holds true. Let now $w_\rho^*(v_\rho^*; \epsilon)$ be the solution of

$$\mathcal{F}(v_\rho^*; w_\rho^*, \rho, \epsilon) = 0,$$

and, in a similar way, let $w^*(v^*; \epsilon)$ be the solution of

$$\mathcal{F}(v^*; w^*, 0, \epsilon) = 0.$$

Lemma 3.3. *There exists ρ^* and ϵ^* and a constant C_2 such that, for $|\rho| < \rho^*$ and $\epsilon < \rho^2 \epsilon^*$ one has*

$$\|w_\rho^*(v_\rho^*; \epsilon) - w^*(v^*; \epsilon)\|_{\ell^2} < C_2 \rho^2. \quad (53)$$

¹¹This is a delicate point and involves the preservation of a symmetry under the Lyapunov-Schmidt reduction. The equivariance of equation (36) reflects the Gauge invariance of the corresponding Hamiltonian: this is a common variational interpretation of the Kernel equation in the first LS reduction (see [4]). At a second stage, if the Kernel and Range projections commute with the symmetry, then also (47) is equivariant and it is enough to restrict to the transversal directions.

Proof: As in the proof of the previous Lemma, it is possible to show that

$$\mathcal{F}_H(v_\rho^*; h + k, \rho, \epsilon) - F_H(v^*; h + k, \epsilon) = \mathcal{O}(\rho^2);$$

then, again from (42) one can deduce

$$\|h(v_\rho^*; k, \rho, \epsilon) - h(v^*; k, \epsilon)\| < C\rho^2, \quad (54)$$

which combined with (52) gives the desired estimate. \square

Going back to (27), let $\mathbf{v}^*(\rho, \epsilon, \tau)$ and $\mathbf{v}^*(0, \epsilon, \tau')$ be the scaled real solutions (belonging to the Kernel V_2) built respectively with $\phi_\rho^*(\epsilon) = v_\rho^* + w_\rho^*(v_\rho^*; \epsilon)$ and $\phi^*(\epsilon) = v^* + w^*(v^*; \epsilon)$, and

$$u^*(\rho, \epsilon, \tau) = \mathbf{v}^*(\rho, \epsilon, \tau) + \mathbf{w}(\mathbf{v}^*(\rho, \epsilon, \tau), \epsilon), \quad (55)$$

the reconstructed solution of the original perturbed problem (23). Following the same steps developed in [3] one gets (38).

3.5.2. Proof of Theorem 3.2

The proof of Theorem 3.2 is essentially based on a necessary condition for the solvability of the bifurcation equation which is shown to be violated. Precisely, as before, we first show that the same property is violated in the dNLS model (3) and then we extend the result to the system under investigation. Let v^* represent an element of the families (12) with $\varphi \notin \{0, \pi\}$. The first step — deferred to Section 4.2 — consists in showing that the linearized bifurcation equation of the dNLS system ($\rho = 0$)

$$\epsilon \partial_\epsilon P(v^*; 0, 0) + D_k P(v^*; 0, 0)[k] = 0$$

cannot be solved, because the necessary condition

$$\partial_\epsilon P(v^*; 0, 0) \in \text{Range}(D_k P(v^*; 0, 0))$$

does not hold. Once the above is proven, as a consequence, the whole nonlinear equation cannot be solved for (k, ϵ) close to the origin, thus v^* cannot represent a bifurcation point. The last implication, namely the relationship between the linearized equation and the nonlinear equation, can be understood again in terms of bifurcation theory, and is included in the more general statement of Proposition 2.10 of [32] (remark that, using the notation as in [32], in the zigzag case $g^{(2)}(\theta^*) \neq 0$). In qualitative terms, the main idea is that if $\partial_\epsilon P(v^*; 0, 0) \neq 0$ and the linearized equation cannot be solved, then close enough to the origin $P(v^*; k, \epsilon) \neq 0$, since higher order corrections are negligible.

To add some details, one can follow Lemma 4.4 and Remark 4.4 of [37], where a similar condition on the second order term $\partial_\epsilon^2 P(\varphi^*, k_g, 0, 0)$ can be derived for $\partial_\epsilon P(\varphi^*, k_g, 0, 0) = 0$. In brief, one can implement a further Lyapunov-Schmidt decomposition, by splitting again the (four dimensional) space into the subspace $\text{Ker}(D_k P(v^*; 0, 0))$, given by the tangent directions to the φ -family and the Gauge-symmetry, and the remaining $\text{Range}(D_k P(v^*; 0, 0))$. In terms of variables, one simply introduces $k_{\mathcal{K}}$ and $k_{\mathcal{R}}$, the set of coordinates of $\text{Ker}(D_k P(v^*; 0, 0))$ and $\text{Range}(D_k P(v^*; 0, 0))$, respectively, such that $k = k_{\mathcal{K}} + k_{\mathcal{R}}$. After Taylor-expanding and projecting the equation $P(v^*; k_{\mathcal{K}}, k_{\mathcal{R}}, \epsilon) = 0$ onto the Range, one immediately realizes that $k_{\mathcal{R}} = \mathcal{O}(\epsilon)$. Thus, at leading order in the Kernel equation one has

$$\Pi_{\mathcal{K}}[\partial_\epsilon P(v^*; 0, 0)] = 0$$

which is equivalent to

$$\partial_\epsilon P(v^*; 0, 0) \in \text{Range}(D_k P(v^*; 0, 0)).$$

By continuity in ρ , the same conclusions can be derived in the regime of small ρ via the equation

$$\epsilon \partial_\epsilon P_\rho(v_\rho^*; 0, \rho, 0) + D_k P_\rho(v_\rho^*; 0, \rho, 0)[k] = 0$$

due to the following

Proposition 3.2. *Let v_ρ^* as in (51). If the corresponding v^* is such that*

$$\partial_\epsilon P(v^*; 0, 0) \neq 0 \wedge \partial_\epsilon P(v^*; 0, 0) \notin \text{Ker}(D_k P(v^*; 0, 0)), \quad (56)$$

then there exists ρ^* such that, for $|\rho| < \rho^*$ one has

$$\partial_\epsilon P_\rho(v_\rho^*; 0, \rho, 0) \neq 0 \wedge \partial_\epsilon P_\rho(v_\rho^*; 0, \rho, 0) \notin \text{Ker}(D_k P_\rho(v_\rho^*; 0, \rho, 0)).$$

As previously said, this Proposition shows that, also for the Klein-Gordon model, the nonlinear equation cannot be solved for (k, ϵ) close to the origin, therefore v^* cannot represent a bifurcation point.

3.6. A note on the more degenerate model: \mathcal{H}_{101}

The technique developed in this Section is not sufficient to deal with the more degenerate model examined in Section 2.3, i.e., \mathcal{H}_{101} in (14). Actually this kind of degeneracy in a dNLS model was already examined systematically in [37], where we were able to prove the nonexistence of any four-sites phase-shift discrete soliton for ϵ small enough. The crucial point is that the higher non-degeneracy required the analysis of higher order expansions of the Bifurcation Equation: this is exactly the reason that prevents the application of the techniques used in the present paper. Indeed the small perturbation due to the energy, which “measures” the distance among the model (14) and its dNLS-type normal form (16), could be enough to introduce small linear terms in the bifurcation equation allowing for non-trivial solutions, which otherwise would not exist. This, however, depends on the magnitude of the linear term in ϵ introduced by the perturbation. Since the obstruction to nonexistence comes out from the ϵ^2 term in the Kernel equation, the corrections of order ρ^2 would not be relevant for $\rho^2 \ll \epsilon$. However, as we are considering the regime $\epsilon \lesssim \rho^2$ (due to our initial scaling (40)), we cannot exclude the existence of solutions for the perturbed problem.

4. Nonexistence results for the zigzag-dNLS model

In the present Section we give the nonexistence results for the corresponding dNLS model upon which are based the proofs of the previous Section. Since we will closely follow the scheme of [37], many details will be omitted.

Let us rewrite explicitly the model we consider here, i.e.,

$$\omega \phi_j = -\frac{\epsilon}{2} [(\Delta_1 + \Delta_2)\phi]_j + \frac{3}{4} \phi_j |\phi_j|^2, \quad \text{where } \omega := \lambda - 1, \quad (57)$$

and consider the unperturbed solutions

$$\phi_j^{(0)} = \begin{cases} R e^{i\theta_j}, & j \in S, \\ 0, & j \notin S, \end{cases} \quad (58)$$

where $S = \{1, 2, 3, 4\}$ and $R > 0$.

4.1. C^1 nonexistence result

We first state a finite regularity nonexistence result. For this purpose, we assume to deal with a continuation $\{\phi_j(\epsilon)\}_{j \in \mathbb{Z}}$ which is at least C^1 in ϵ . Hence we expand the solution variables ϕ_j in ϵ

$$\phi_j = \phi_j^{(0)} + \epsilon \phi_j^{(1)} + o(\epsilon), \quad (59)$$

where $o(\epsilon)$ is a continuous function. The continuation is assumed to be performed at fixed period (frequency). With the perturbative approach, we are able to prove

Theorem 4.1. *For ϵ small enough, the only unperturbed solutions (58) that can be continued to C^1 solutions $\phi(\epsilon)$ of (57), (with $\epsilon \neq 0$), correspond to $\varphi_j \in \{0, \pi\}$.*

In the proof of the above Theorem, a key point is the fact that the discrete map (57) preserves

$$J_j := \Im \left(\phi_{j-1} \bar{\phi}_j + \phi_{j-2} \bar{\phi}_j + \phi_{j-1} \bar{\phi}_{j+1} \right). \quad (60)$$

The conservation of this quantity, the so-called *current*, $J_j \equiv J$, together with the hypothesis $\{\phi_j\}_{j \in \mathbb{Z}} \in \ell^2(\mathbb{C})$, imply

$$J_j = 0, \quad \forall j \in \mathbb{Z}. \quad (61)$$

As in our previous paper, in what follows we take a look at the general structure of the expansion, in the present case up to order one, of both the equations and the conserved quantity; moreover, from the zero order expansion, we determine the candidate solutions.

The strategy is then to investigate directly such equations evaluated into the candidate solutions; and to exclude all the solutions prohibited by Theorem 4.1 looking for the incompatibility of the conserved quantity with the equations.

4.1.1. Zero-order expansion and candidate solutions

The stationary equation (57) at order zero gives the uncoupled system

$$\omega \phi_j^{(0)} = \frac{3}{4} \phi_j^{(0)} \left| \phi_j^{(0)} \right|^2, \quad (62)$$

which is invariant under the action of $e^{i\tau}$. By using (58), it provides the frequency λ of the orbit, and its detuning ω from the linear frequency 1, namely

$$\omega = \frac{3}{4} R^2 \quad \text{and} \quad \lambda = 1 + \frac{3}{4} R^2. \quad (63)$$

The conservation law (61) at order zero gives

$$J_j^{(0)} := \Im \left(\phi_{j-1}^{(0)} \bar{\phi}_j^{(0)} + \phi_{j-2}^{(0)} \bar{\phi}_j^{(0)} + \phi_{j-1}^{(0)} \bar{\phi}_{j+1}^{(0)} \right) = 0. \quad (64)$$

If we take only 4 oscillators not at rest (as in our ansatz (58)), then (64) is identically satisfied for $j \leq 0$ and $j \geq 5$. For the remaining variables site $j \in \mathcal{S}$, by recalling the definition $\varphi_j := \theta_{j+1} - \theta_j$ of the phase-differences as in (6), equations (64) give

$$\begin{aligned} \sin(\varphi_1) &= -\sin(\varphi_1 + \varphi_2), \\ \sin(\varphi_2) &= \sin(\varphi_1) + \sin(\varphi_3), \\ \sin(\varphi_3) &= -\sin(\varphi_2 + \varphi_3). \end{aligned} \quad (65)$$

Remark 4.1. *The above system of equations for the phase-differences coincides with (9) and (11).*

As already anticipated in Section 2, the solutions of the system (65) provide the two families $F_1 : \boldsymbol{\varphi} = (\varphi, \pi, -\varphi)$ and $F_2 : \boldsymbol{\varphi} = (\varphi, \pi, \varphi + \pi)$, respectively (see (12)). Their intersections give the two phase-shift solutions $F_1 \cap F_2 = \Phi^{(sv)} = \pm(\frac{\pi}{2}, \pi, -\frac{\pi}{2})$, while they include some in/out-of-phase solutions, i.e., $\{(0, \pi, 0), (\pi, \pi, \pi)\} \in F_1$ and $\{(0, \pi, \pi), (\pi, \pi, 0)\} \in F_2$. The remaining possible in/out-of-phase solutions (those with $\varphi_2 = 0$) are not included in the above families, i.e., $F_{\text{iso}} : \boldsymbol{\varphi} = \{(0, 0, 0), (0, 0, \pi), (\pi, 0, 0), (\pi, 0, \pi)\}$.

4.1.2. First order expansions

The first order expansions of both the stationary equation (57) and the density current (60) are easily deduced and take the form

$$\begin{aligned} \omega \phi_j^{(1)} &= -\frac{1}{2} \left[\phi_{j+2}^{(0)} + \phi_{j+1}^{(0)} + \phi_{j-1}^{(0)} + \phi_{j-2}^{(0)} \right] + 2\phi_j^{(0)} \\ &\quad + \frac{3}{4} \left[2\phi_j^{(1)} \left| \phi_j^{(0)} \right|^2 + \left(\phi_j^{(0)} \right)^2 \bar{\phi}_j^{(1)} \right]; \end{aligned} \quad (66)$$

$$\begin{aligned} 0 &= \Im \left(\phi_{j-1}^{(0)} \bar{\phi}_j^{(1)} + \phi_{j-2}^{(0)} \bar{\phi}_j^{(1)} + \phi_{j-1}^{(0)} \bar{\phi}_{j+1}^{(1)} \right. \\ &\quad \left. + \phi_{j-1}^{(1)} \bar{\phi}_j^{(0)} + \phi_{j-2}^{(1)} \bar{\phi}_j^{(0)} + \phi_{j-1}^{(1)} \bar{\phi}_{j+1}^{(0)} \right). \end{aligned} \quad (67)$$

4.1.3. Second order expansion and conclusion

To get the nonexistence result, the solutions of the equations are inserted into the conserved current.

Starting with the two families of asymmetric vortex solutions, F_1 and F_2 , with the exclusion of the F_{iso} and $\Phi^{(sv)}$ solutions, we end up, for the first family, with the following set of linear equations

$$\begin{aligned} B + C &= 2 \sin \varphi \\ (1 + \cos \varphi)(B + C) + \cos^2 \varphi(A + D) &= 0 \\ B + C &= -2 \sin \varphi \end{aligned} \quad (68)$$

where A, B, C, D are left free at previous order. The system is clearly impossible once we exclude $\varphi = 0, \pi$. The second family is treated in the same way.

Concerning the symmetric vortex solutions $\Phi^{(sv)}$, by similar calculations we have again that the conservation law at order zero is identically satisfied, and at order one is equivalent to

$$4i = 0, \quad B + C = 0, \quad -4i = 0, \quad (69)$$

which is impossible independently of the four free parameters left from the equation.

4.2. C^0 nonexistence result

Following again [37], we want to complete the nonexistence result to C^0 solutions. The strategy is based on a Lyapunov-Schmidt decomposition, where suitable expansions are performed mainly at the level of the (regular) equations, without assumptions on the regularity of the solutions. We recall that this stronger result is technically needed, as already mentioned in the proof of Theorem 3.2, in order to obtain the similar result for the Klein-Gordon model in the small energy regime: in

fact, we are going to show here that condition (56) assumed in Proposition 3.2 holds true. However, since the scheme is exactly the same of [37], we only sketch the key points. The main difference is that in such a paper we considered the case H_{101} while here we are dealing with the case H_{110} , so that

$$L := \Delta_1 + \Delta_2 .$$

The key part of the analysis is in the bifurcation (kernel) equation, and in the application of Lemma 4.4 and Remark 4.4 of [37]; to this purpose we check the projection of

$$\partial_\epsilon P(v^*, 0, 0) = \Pi_K L h^{(1,0)}(v^*, 0, 0) ,$$

where

$$h^{(1,0)}(v^*, 0, 0) := -\Lambda^{-1} \Pi_H L v^*$$

onto the Kernel of the differential operator

$$D_k P(v^*, 0, 0)[k] = \Pi_K L k - \frac{3}{2} \Re(v^* \overline{h^{(1,0)}}) k ,$$

where v^* is in one of the families F_1 and F_2 , and Π_K and Π_H are the projectors onto respectively the Kernel and the Range of Λ . We deal explicitly with one family only; taking $F_1 : \varphi = (\varphi, \pi, -\varphi)$, and setting $\theta_0 = 0$, we have $\theta = (0, \varphi, \pi + \varphi, \pi)$, which gives the following representation of v^* in complex variables

$$v^* \Big|_S (\varphi) = R(1, e^{i\varphi}, -e^{i\varphi}, -1) .$$

As a consequence, the Kernel's basis reads

$$e_j \Big|_S = iR\{(1, 0, 0, 0), (0, e^{i\varphi}, 0, 0), (0, 0, -e^{i\varphi}, 0), (0, 0, 0, -1)\} .$$

An easy computation gives Lv^* , precisely

$$\left[\dots, 0, 1, 1 + e^{i\varphi} \Big| -4, -5e^{i\varphi}, 5e^{i\varphi}, 4 \Big| - (1 + e^{i\varphi}), -1, 0, \dots \right] ;$$

using the scalar product $\Pi_K L v^* = \sum_{j=1}^4 \Re(Lv^* \overline{e_j}) e_j$, one gets $\Pi_K L v^* = 0$, since $\Re(Lv^* \overline{e_j}) = 0$ for all $j = 1, \dots, 4$. Hence $\Pi_H L v^* = Lv^*$. Since

$$\Lambda h = \begin{cases} -2\omega h , & j \in S \\ \omega h , & j \notin S \end{cases} ,$$

then $-\Lambda^{-1} \Pi_H L v^*$ takes the form

$$\frac{1}{\omega} \left[\dots, 0, -1, -(1 + e^{i\varphi}) \Big| -2, -\frac{5}{2}e^{i\varphi}, \frac{5}{2}e^{i\varphi}, 2 \Big| (1 + e^{i\varphi}), 1, 0, \dots \right] .$$

Given that our last operation is a projection onto the Kernel, we limit the next computation on the core sites, precisely $-(\Lambda^{-1} \Pi_H L v^*) \Big|_S$ reads

$$\frac{1}{\omega} \left[6 - e^{i\varphi}, \frac{23}{2}e^{i\varphi} - 1, -\frac{23}{2}e^{i\varphi} + 1, -6 + e^{i\varphi} \right] .$$

We finally get

$$\partial_\epsilon P(v^*, 0, 0) = -i \sin(\varphi) \left[0 \Big| 1, -e^{i\varphi}, e^{i\varphi}, -1 \Big| 0 \right] .$$

Upon verifying that the four-dimensional matrix representing the linear operator $D_k P(v^*, 0, 0)[k]$ has rank 2, we know for free the Kernel generators, since the Gauge direction and the

direction tangent to the family for sure belong to it; these are respectively

$$\partial_\varphi v^*(\varphi) = \left[0 \Big| 0, ie^{i\varphi}, -ie^{i\varphi}, 0 \Big| 0 \right] , \quad \partial_{\theta_0} e^{i\theta_0} v^*(\varphi) = ie^{i\theta_0} v^*(\varphi) .$$

Since the Gauge symmetry is preserved along the whole construction, we have $\partial_\epsilon P \perp \partial_{\theta_0} e^{i\theta_0} v^*$, which can even be checked by the direct computation of $\partial_{\theta_0} e^{i\theta_0} v^*(\varphi) \cdot \partial_\epsilon P(v^*, 0, 0) = 0$. The other scalar product gives instead

$$\begin{aligned} \partial_\varphi v^*(\varphi) \cdot \partial_\epsilon P(v^*, 0, 0) &= -\sin(\varphi) \left[\Re\left(ie^{i\varphi}(ie^{-i\varphi})\right) \right. \\ &\quad \left. + \Re\left(-ie^{i\varphi}(-ie^{-i\varphi})\right) \right] \\ &= 2 \sin(\varphi) , \end{aligned}$$

which is different from zero, apart from the cases $\varphi = 0, \pi$. Thus, we can conclude that the projection of $\partial_\epsilon P(v^*(\varphi), 0, 0)$ onto the Kernel of $D_k P(v^*, 0, 0)$ is different from zero on any phase-shift discrete soliton considered in the family. This represents a sufficient condition for nonexistence of the continuation.

5. Conclusions - Future Directions

The present paper represents a natural follow up of [37], where we studied the related problem of the nonexistence of degenerate phase-shift discrete solitons in a non-local dNLS lattice. We recall that in [37] the nonexistence of phase-shift discrete solitons, which was not easily achievable by means of averaging methods due to the degeneracy of the problem, was obtained in an efficient way exploiting the rotational symmetry of the model and the density current conservation along the spatial profile of any candidate soliton. The absence of these ingredients in Klein-Gordon models represents an additional layer of difficulty to the degeneracy that one has to face in the continuation problem that we here address.

Keeping in mind the connections among these two classes of Hamiltonian models (KG and dNLS), a natural (although indirect) way to proceed is to transfer the results which are accessible in the dNLS context to similar results which are expected to be valid in the KG context, keeping track of the relevant correction terms. In this work we examined mainly KG systems with interactions beyond nearest neighbors interactions (bearing also in mind connections with higher dimensional lattices), focusing principally on the zigzag model for our analytical considerations. In this model, by means of Lyapunov-Schmidt techniques, we showed that that this approach actually works provided some smallness assumptions are made on the main physical parameters of the models: the energy E and the coupling strength ϵ .

However, the strategy presented here, is based on a first order normal form approximation of the KG model, and thus it has some limitations in cases where higher order degeneracies occur. In order to showcase this fact we shortly examine a model that exhibits next-to-next nearest neighbors interactions namely the \mathcal{H}_{01} model. Although the previously described methodology cannot be applied, the numerical exploration performed in the Section 2.3 shows elements which strongly overlap with those that one can obtain in the corresponding dNLS normal form H_{101} , for which a rigorous answer has been given already in [37]. This naturally leads us to conjecture that a corresponding nonexistence statement of phase-shift four-sites multibreathers holds true also for \mathcal{H}_{101} .

In order to prove such a conjecture, one could still follow this indirect approach by increasing the accuracy of the normal form approximation by adding further non-local linear and nonlinear terms to the dNLS H_{101} , in the spirit of a more general dNLS approximation (see [30, 31]). Alternatively, one can use a more direct approach and perform a local normal form technique around the low-dimensional resonant torus, with the advantage of working directly in the original KG model without passing from the dNLS approximation (see [36] for the maximal tori case). With this scheme we expect to derive a normal form which naturally extends the effective Hamiltonian method introduced in [1]. In any case, and whatever the perturbation method one prefers to apply may be, it appears natural that the accuracy required in the approximation is directly related to the order of the degeneracy of the problem: hence, for highly degenerate problems the help of a computer assisted manipulation may be unavoidable and the choice of the method can become extremely relevant.

A related comment is that in the present work we have limited our considerations to one-dimensional settings with long-range interactions. Extending relevant ideas to genuinely higher-dimensional KG settings, where again the understanding built on the basis of the dNLS [32, 18] may be useful, is another natural avenue for future work.

Acknowledgements

The authors, V.K., P.G.K., acknowledge that this work made possible by NPRP grant # [9-329-1-067] from Qatar National Research Fund (a member of Qatar Foundation). The findings achieved herein are solely the responsibility of the authors.

- [1] T. Ahn, R.S. MacKay, and J.-A. Sepulchre. Dynamics of relative phases: Generalised multibreathers. *Nonlinear Dynamics*, 25(1-3):157–182, 2001. cited By 23.
- [2] Antonio Ambrosetti and Giovanni Prodi. *A primer of nonlinear analysis*. Cambridge University Press, Cambridge, 1995. Corrected reprint of the 1993 original.
- [3] Dario Bambusi, Simone Paleari, and Tiziano Penati. Existence and continuous approximation of small amplitude breathers in 1D and 2D Klein-Gordon lattices. *Appl. Anal.*, 89(9):1313–1334, 2010.
- [4] Massimiliano Berti. *Nonlinear oscillations of Hamiltonian PDEs*. Progress in Nonlinear Differential Equations and their Applications, 74. Birkhäuser Boston, Inc., Boston, MA, 2007.
- [5] P. Binder, D. Abraimov, A. V. Ustinov, S. Flach, and Y. Zolotaryuk. Observation of breathers in josephson ladders. *Phys. Rev. Lett.*, 84:745–748, Jan 2000.
- [6] N. Boechler, G. Theoharis, S. Job, P. G. Kevrekidis, Mason A. Porter, and C. Daraio. Discrete breathers in one-dimensional diatomic granular crystals. *Phys. Rev. Lett.*, 104:244302, Jun 2010.
- [7] D. K. Campbell, S. Flach, and Yu. S. Kivshar. Localizing energy through nonlinearity and discreteness. *Physics Today*, 57:43–49, 2004.
- [8] C. Chong, R. Carretero-González, B. A. Malomed, and P. G. Kevrekidis. Variational approximations in discrete nonlinear Schrödinger equations with next-nearest-neighbor couplings. *Phys. D*, 240(14-15):1205–1212, 2011.
- [9] C. Chong, F. Li, J. Yang, M. O. Williams, I. G. Kevrekidis, P. G. Kevrekidis, and C. Daraio. Damped-driven granular chains: An ideal playground for dark breathers and multibreathers. *Phys. Rev. E*, 89:032924, Mar 2014.
- [10] Thierry Cretegny and Serge Aubry. Spatially inhomogeneous time-periodic propagating waves in anharmonic systems. *Phys. Rev. B*, 55:R11929–R11932, May 1997.
- [11] J. Cuevas, L. Q. English, P. G. Kevrekidis, and M. Anderson. Discrete breathers in a forced-damped array of coupled pendula: Modeling, computation, and experiment. *Phys. Rev. Lett.*, 102:224101, Jun 2009.
- [12] J. Cuevas, V. Koukouloyannis, P. G. Kevrekidis, and J. F. R. Archilla. Multibreather and vortex breather stability in klein-gordon lattices: equivalence between two different approaches. *International Journal of Bifurcation and Chaos*, 21(08):2161–2177, 2011.
- [13] Nikos K. Efremidis and Demetrios N. Christodoulides. Discrete solitons in nonlinear zigzag optical waveguide arrays with tailored diffraction properties. *Phys. Rev. E*, 65:056607, May 2002.
- [14] L. Q. English, R. Basu Thakur, and Ryan Stearrett. Patterns of traveling intrinsic localized modes in a driven electrical lattice. *Phys. Rev. E*, 77:066601, Jun 2008.
- [15] S. Flach, K. Kladko, and R. S. MacKay. Energy thresholds for discrete breathers in one-, two-, and three-dimensional lattices. *Phys. Rev. Lett.*, 78:1207–1210, Feb 1997.
- [16] Sergej Flach and Andrey V. Gorbach. Discrete breathers advances in theory and applications. *Physics Reports*, 467(1):1 – 116, 2008.
- [17] Todd Kapitula. Stability of waves in perturbed Hamiltonian systems. *Phys. D*, 156(1-2):186–200, 2001.
- [18] Panayotis G. Kevrekidis. *The discrete nonlinear Schrödinger equation*, volume 232 of *Springer Tracts in Modern Physics*. Springer-Verlag, Berlin, 2009. Mathematical analysis, numerical computations and physical perspectives.
- [19] P.G. Kevrekidis. Non-nearest-neighbor interactions in nonlinear dynamical lattices. *Physics Letters, Section A: General, Atomic and Solid State Physics*, 373(40):3688–3693, 2009. cited By 5.
- [20] P.G. Kevrekidis, D.J. Frantzeskakis, and R. Carretero-González. *Emergent Nonlinear Phenomena in Bose-Einstein Condensates*. Springer Series on Atomic, Optical and Plasma Physics. Springer-Verlag, Heidelberg, 2008.
- [21] V Koukouloyannis, P G Kevrekidis, K J H Law, I Kourakis, and D J Frantzeskakis. Existence and stability of multisite breathers in honeycomb and hexagonal lattices. *Journal of Physics A: Mathematical and Theoretical*, 43(23):235101, 2010.
- [22] V. Koukouloyannis, P. G. Kevrekidis, K. J. H. Law, I. Kourakis, and D. J. Frantzeskakis. Existence and stability of multisite breathers in honeycomb and hexagonal lattices. *J. Phys. A*, 43(23):235101, 16, 2010.
- [23] V. Koukouloyannis, P.G. Kevrekidis, J. Cuevas, and V. Rothos. Multibreathers in Klein-Gordon chains with interactions beyond nearest neighbors. *Phys. D*, 242(1):16 – 29, 2013.
- [24] Vassilis Koukouloyannis. Non-existence of phase-shift breathers in one-dimensional Klein-Gordon lattices with nearest-neighbor interactions. *Phys. Lett. A*, 377(34-36):2022–2026, 2013.
- [25] Vassilis Koukouloyannis and Simos Ichtarioglou. Existence of multibreathers in chains of coupled one-dimensional Hamiltonian oscillators. *Phys. Rev. E (3)*, 66(6):066602, 8, 2002.
- [26] Vassilis Koukouloyannis and Panayotis G. Kevrekidis. On the stability of multibreathers in Klein-Gordon chains. *Nonlinearity*, 22(9):2269–2285, 2009.
- [27] Vassilis Koukouloyannis and MacKay Robert S. Existence and stability of 3-site breathers in a triangular lattice. *J. Phys. A*, 38(5):1021 – 1030, 2005.
- [28] Falk Lederer, George I. Stegeman, Demetri N. Christodoulides, Gaetano Assanto, Moti Segev, and Yaron Silberberg. Discrete solitons in optics. *Physics Reports*, 463(1):1 – 126, 2008.
- [29] R S MacKay and S Aubry. Proof of existence of breathers for time-reversible or hamiltonian networks of weakly coupled oscillators. *Nonlinearity*, 7(6):1623, 1994.
- [30] Simone Paleari and Tiziano Penati. An extensive resonant normal form for an arbitrary large Klein-Gordon model. *Ann. Mat. Pura Appl. (4)*, 195(1):133–165, 2016.
- [31] Simone Paleari and Tiziano Penati. Long time stability of small-amplitude breathers in a mixed FPU-KG model. *Z. Angew. Math. Phys.*, 67(6):Art. 148, 21, 2016.
- [32] D. E. Pelinovsky, P. G. Kevrekidis, and D. J. Frantzeskakis. Persistence and stability of discrete vortices in nonlinear

- Schrödinger lattices. *Phys. D*, 212(1-2):20–53, 2005.
- [33] D. E. Pelinovsky, P. G. Kevrekidis, and D. J. Frantzeskakis. Stability of discrete solitons in nonlinear Schrödinger lattices. *Phys. D*, 212(1-2):1–19, 2005.
- [34] Dmitry Pelinovsky, Tiziano Penati, and Simone Paleari. Approximation of small-amplitude weakly coupled oscillators by discrete nonlinear Schrödinger equations. *Rev. Math. Phys.*, 28(7):1650015, 25, 2016.
- [35] Dmitry Pelinovsky and Anton Sakovich. Multi-site breathers in Klein-Gordon lattices: stability, resonances and bifurcations. *Nonlinearity*, 25(12):3423–3451, 2012.
- [36] T. Penati, M. Sansottera, and V. Danesi. A normal form method for the continuation of periodic orbits on completely resonant maximal tori. *Communications in Nonlinear Science and Numerical Simulation*, page 10.1016/j.cnsns.2018.02.003, 2018.
- [37] T. Penati, M. Sansottera, S. Paleari, V. Koukouloyannis, and P.G. Kevrekidis. On the nonexistence of degenerate phase-shift discrete solitons in a dNLS nonlocal lattice. *Physica D - Nonlinear Phenomena*, page 10.1016/j.physd.2017.12.012, 2017.
- [38] M. Sato, B. E. Hubbard, L. Q. English, A. J. Sievers, B. Ilic, D. A. Czaplewski, and H. G. Craighead. Study of intrinsic localized vibrational modes in micromechanical oscillator arrays. *Chaos: An Interdisciplinary Journal of Nonlinear Science*, 13(2):702–715, 2003.
- [39] M. Sato, B. E. Hubbard, A. J. Sievers, B. Ilic, D. A. Czaplewski, and H. G. Craighead. Observation of locked intrinsic localized vibrational modes in a micromechanical oscillator array. *Phys. Rev. Lett.*, 90:044102, Jan 2003.
- [40] U. T. Schwarz, L. Q. English, and A. J. Sievers. Experimental generation and observation of intrinsic localized spin wave modes in an antiferromagnet. *Phys. Rev. Lett.*, 83:223–226, Jul 1999.
- [41] E. Trias, J. J. Mazo, and T. P. Orlando. Discrete breathers in nonlinear lattices: Experimental detection in a josephson array. *Phys. Rev. Lett.*, 84:741–744, Jan 2000.